iScience

CellPress
OPEN ACCESS

Article

Comprehensive analysis of the relationship between xanthine oxidoreductase activity and chronic kidney disease

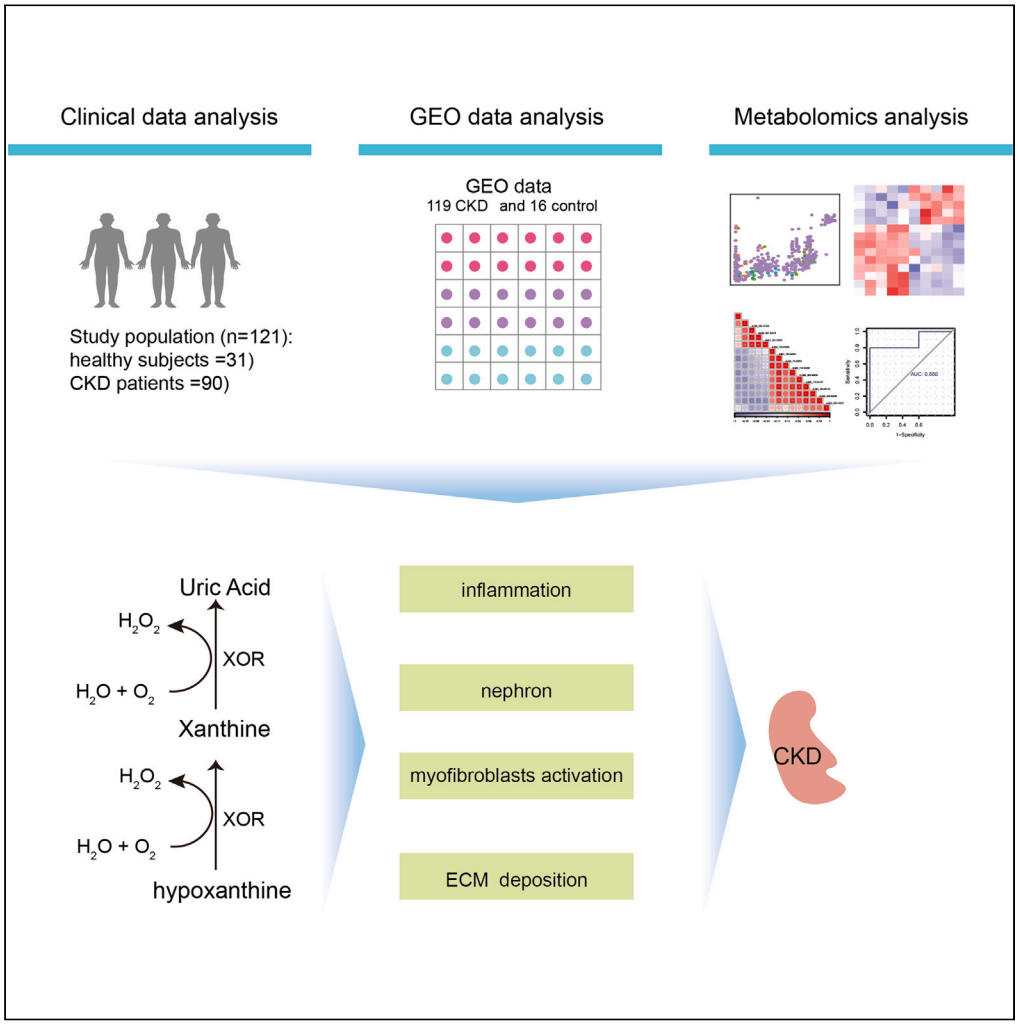

Yiyuan Zhang, Xiaobao Ding, Lihao Guo, ..., Yong Xu, Hailun Li, Donghui Zheng

haeyxy@163.com (Y.X.)
lihailun1o1@sina.com (H.L.)
zddwjj@126.com (D.Z.)

Highlights

XOR activity was increased in CKD patients, closely associated with disease severity

LASSO logistic regression and random forest can identify XDH based on GEO datasets

Purine metabolites, which generated by XOR were upregulated by TGF-β in HK2 cells

XOR might be involved in the process of CKD by generating xanthine

Zhang et al., iScience 26, 107332
November 17, 2023
https://doi.org/10.1016/j.isci.2023.107332

iScience

CellPress
OPEN ACCESS

Article

Comprehensive analysis of the relationship between xanthine oxidoreductase activity and chronic kidney disease

Yiyuan Zhang,[1,3] Xiaobao Ding,[1,2,3] Lihao Guo,[1] Yanan Zhong,[1] Juan Xie,[1] Yong Xu,[1,*] Hailun Li,[1,*] and Donghui Zheng[1,4,*]

SUMMARY

Chronic kidney disease (CKD) is a common disease that seriously endangers human health. However, the potential relationship between xanthine oxidoreductase (XOR) activity and CKD remains unclear. In this study, we used clinical data, CKD datasets from the Gene Expression Omnibus database, and untargeted metabolomics to explain the relationship between XOR activity and CKD. First, XOR activity showed high correlation with the biomarkers of CKD, such as serum creatinine, blood urea nitrogen, uric acid, and estimated glomerular filtration rate. Then, we used least absolute shrinkage and selection operator logical regression algorithm and random forest algorithm to screen CKD molecular markers from differentially expressed genes, and the results of qRT-PCR of XDH, KOX-1, and ROMO1 were in accordance with the results of bioinformatics analyses. In addition, untargeted metabolomics analysis revealed that the purine metabolism pathway was significantly enriched in CKD patients in the simulated models of kidney fibrosis.

INTRODUCTION

Xanthine oxidoreductase (XOR) is a complex molybdenum protein polymer that has been known for more than 100 years.[1] In mammals, XOR mainly catalyzes the last two steps of purine metabolism, including catalysis of hypoxanthine to xanthine and conversion of xanthine to uric acid. The enzyme has two interconvertible forms, including one with dehydrogenase activity (XDH) and another one with oxidase activity (XO).[2] In normal physiological conditions, XOR is predominantly present in the dehydrogenase form and uses NAD+ as its preferred electron acceptor to yield NADH and produce uric acid (UA) simultaneously. The XO form simultaneously produces UA and reactive oxygen species (ROS) by using oxygen.[3] Therefore, the activity of XOR is the sum of the two existing forms. Hypoxia, inflammation, and ischemia-reperfusion injury increase XOR activity, which can increase the production of ROS. The ROS produced by XOR during the reaction process can damage the function of endothelial cells and activate inflammasomes.[4,5]

Considering the increasing prevalence, poor outcome, and economic burden, chronic kidney disease (CKD), which affects approximately 13.4% of general population, has been reported to be a significant public health issue with an annual growth rate of 8%.[6,7] The pathogenesis of CKD is associated with age and sex,[8] diabetes and obesity,[9,10] poorly controlled arterial hypertension,[11] monogenic kidney disease,[12] congenital abnormalities,[13] climate,[14] infections and chronic inflammation,[15] malignancy,[16] episodes of acute kidney injury,[17,18] and low nephron endowment at birth.[19] Assessment of kidney damage (proteinuria) and estimation of renal function (estimated glomerular filtration rate, eGFR) are two routine clinical biomarker assessments for CKD.[20] In addition, blood urea nitrogen (BUN) level is considered an estimate of renal function in patients with renal disorders.[21–23] Previous studies have pointed out that the kidney as an organ with high metabolic activity is extremely susceptible to damage by ROS.[24,25] In pathological conditions, the balance between oxidants and antioxidants is disrupted, and the antioxidant systems can be overwhelmed. ROS may contribute to many pathological conditions and diseases.[26–28] ROS can also promote the progression of CKD and even contribute to cardiovascular disease (CVD).[27] UA, the end product of XOR, has been reported to be a potential contributory risk factor in the development and progression of CKD. XOR is one of the main sources of ROS.[29] Accruing evidence suggests that XOR inhibitors may provide direct renal benefits owing to their hypouricemic effect, inhibition of the inflammatory response, and

[1]Department of Nephrology, The Affiliated Huai'an Hospital of Xuzhou Medical University and Huai'an Second People's Hospital, Huai'an, China

[2]Department of Pharmacology, Jiangsu Key Laboratory of New Drug Research and Clinical Pharmacy, Xuzhou Medical University, Xuzhou, Jiangsu Province, China

[3]These authors contributed equally

[4]Lead contact

*Correspondence: haeyxy@163.com (Y.X.), lihailun1o1@sina.com (H.L.), zddwjj@126.com (D.Z.)

https://doi.org/10.1016/j.isci.2023.107332

inhibition of oxidative stress. However, it should be noted that the relationship between XOR activity and CKD remains unclear.

Therefore, the aim of this study was to evaluate this relationship by using clinical data, CKD datasets from the GEO database, and untargeted metabolomics. At clinical data level, XOR activity highly correlated with two clinical biomarkers of CKD, such as eGFR and BUN. At transcriptomic level, XDH was identified by screening molecular markers by performing LASSO logistic regression algorithm and random forest based on public GEO datasets. Untargeted metabolomics analysis revealed that the purine metabolism pathway including the metabolite xanthine was significantly enriched in CKD patients in the simulated models of kidney fibrosis. Although additional experiments in human renal biopsy are needed to verify this finding, a new insight into the relationship between XOR activity and CKD was provided in this study.

RESULTS

Profile of clinical data, GEO, and untargeted metabolomics

To investigate the relationship between XOR activity and CKD, we performed integrative analysis to gain insights at multiple levels, including clinical data, CKD datasets from GEO, and untargeted metabolomics (Figure 1). CKD patients were surveyed and filtered for systematic analysis of the relationship between XOR activity and other physiological characteristics such as gender, age, and fasting blood glucose (FBG) (Figure 1A). Public GEO datasets for CKD were collected to screen the hub molecular markers for CKD based on multiple machine learning techniques (Figure 1B). Untargeted metabolomics was performed to obtain the key metabolic pathways in the simulated models of kidney fibrosis (Figure 1C).

Systematic analysis of clinical data of CKD patients

Out of 172 participants, clinical data were obtained for 90 patients and 31 control participants after filtering out individuals with incomplete clinical information. All participants' clinic profiles are shown in Table 1, illustrating that there were significant differences in age, systolic blood pressure, serum creatinine (Scr), FBG, total protein, albumin, red blood cell, white blood cell, hemoglobin, NOD-like receptor thermal protein domain-associated protein 3 (NLRP3), and XOR between the control participants and CKD patients. All CKD patients' underlying kidney disease is shown in Table 2. As shown in Figure 2 and Table S1, we performed Pearson correlation analysis to evaluate the relationship between XOR and other clinical symptoms. In CKD patients, XOR activity showed high positive correlations with FBG, Scr, BUN, UA, and NLRP3, and a negative correlation with eGFR (Figures 2C–2F, Table S1A). XO activity showed high positive correlations with age, FBG, Scr, BUN, and UA, and negative correlation with eGFR (Table S1A). XO/XOR ratio correlated positively with eGFR and negatively with Scr and UA (Table S1A). The relationship between XOR activity and eGFR suggested that XOR activity might be a potential diagnostic marker or a key pathogenicity factor for CKD. Interestingly, in the control participants, XOR activity and XO activity showed negative correlations with UA and NLRP3 (Figures 2A and 2B, Table S1B).

For further study, the CKD patients were divided into two groups according to the eGFR level. For the eGFR<60 mL/(min·1.73 m^2) group, the XOR activity and FBG were more significantly increased, while the XO level was not significantly altered. The NLRP3 level increased significantly in all CKD patients. Given the importance of glycemic control in CKD patients with regard to decreased XOR leading to a decrease in CVD events,[30] the participants were divided into the diabetes and the non-diabetes groups and the results demonstrated that the diabetes group was characterized by increased levels of XOR (Figures 2G–2I). Additionally, for the non-diabetes group, XOR activity showed high negative correlations with eGFR and positive correlations with Scr, BUN, and UA (Table S1). These results indicated that though the XOR activity of CKD patients was affected by diabetes, the XOR activity was related to eGFR, BUN, Scr, and UA, and the trends were consistent, regardless of diabetes status.

Data preprocessing and DEGs screening in CKD

To further investigate whether XOR plays potentially important roles in CKD by distinct modes of action at the molecular level, we first searched and downloaded the gene expression matrix of CKD from the GEO database. In total, 135 samples including 119 CKD patients and 16 healthy subjects were available from five datasets, including GSE15072, GSE45980, GSE66494, GSE69438, and GSE70528 (Figure 3A). Then, inter-batch differences were removed in the merged dataset, and principal component analysis (PCA) was generated for the standardized dataset. As shown in Figure 3B and Table S2, compared with the result

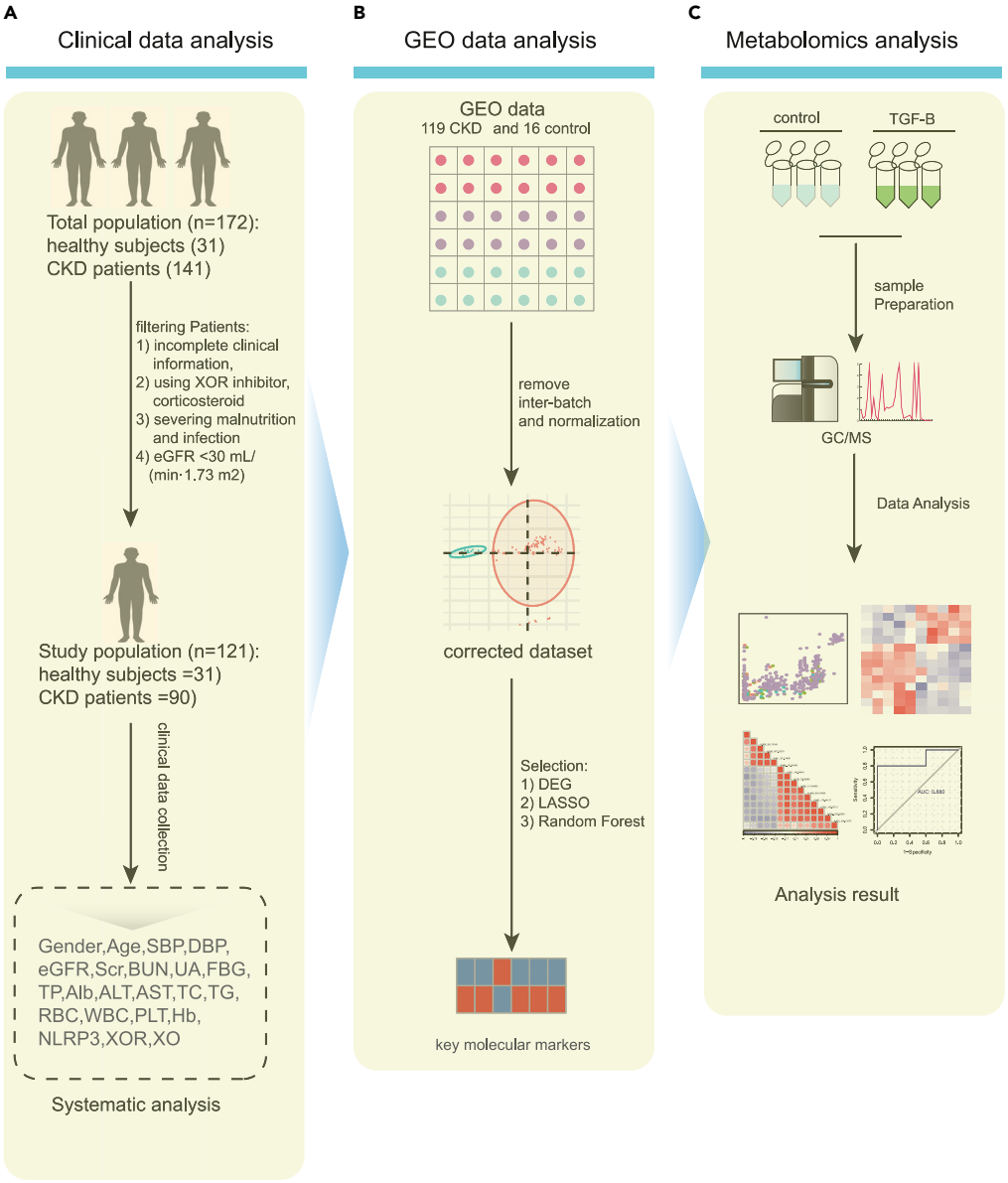

Figure 1. Summary of datasets in this study

(A–C) Schematic diagram for clinical data (A), GEO datasets (B), and untargeted metabolomics (C). Clinical data were obtained from healthy subjects (31) and CKD patients (141). A total of 135 samples including 119 CKD patients and 16 healthy subjects were downloaded for screening differentially expressed genes and molecular markers between the healthy subjects and CKD patients. Untargeted metabolomics analysis was performed for further validation in the simulated models of kidney fibrosis by TGF-β.

of PCA based on the raw data, the CKD and normal control samples clustered separately after correction, indicating that the corrected dataset was reliable. Based on the corrected gene expression matrix, a total of 6048 differentially expressed genes, including 3049 upregulated and 2999 downregulated genes, were identified for subsequent analysis (Figure 3C). Kyoto Encyclopedia of Genes and Genomes (KEGG) enrichment analysis revealed that aldosterone-regulated sodium reabsorption, carbohydrate digestion and absorption, fructose and mannose metabolism, gastric acid secretion, arrhythmogenic right ventricular cardiomyopathy, hypertrophic cardiomyopathy, dilated cardiomyopathy, platelet activation, oxytocin signaling pathway, and ABC transporters were enriched in differentially expressed genes (DEGs) (Figure 3D and Table S2).

Table 1. Baseline characteristics of all participants

	Control participants(n = 31)	CKD patients(n = 90)	*p*
Male/female	17/14	45/45	–
Age (years)	44.90 (20–76)	67 (21–90)	<0.0001
SBP (mmHg)	129.1 ± 19.03	148.4 ± 22.41	<0.0001
DBP (mmHg)	79.03 ± 11.19	81.14 ± 11.95	–
eGFR mL/(min·1.73m^2)	–	78.35 ± 21.86	–
Scr (μmol/L/L)	51.23 ± 10.78	87.02 ± 32.73	<0.0001
BUN (mmol/L)	5.26 ± 0.99	6.01 ± 2.38	–
UA (μmol/L/L)	300.7 ± 56.69	295.8 ± 66.08	–
FBG (mmol/L)	4.95 ± 0.32	5.80 ± 1.41	0.0006
TP (g/L)	74.54 ± 3.74	66.7 ± 8.52	<0.0001
Alb (g/L)	47.17 ± 2.38	39.07 ± 5.17	<0.0001
ALT (IU/L)	19.60 ± 8.31	19.58 ± 9.30	–
AST (IU/L)	18.33 ± 4.27	20.33 ± 6.11	–
TC (mmol/L)	4.37 ± 0.80	4.38 ± 1.42	–
TG (mmol/L)	1.13 ± 0.47	1.52 ± 1.52	–
Male/female	17/14	45/45	–
RBC (×10^{12}/L)	4.72 ± 0.30	4.45 ± 0.62	0.0079
WBC (×10^9/L)	5.921 ± 1.065	6.864 ± 1.961	0.0104
PLT (×10^9/L)	229.6 ± 50.75	205.6 ± 66.33	–
Hb (g/L)	143.4 ± 10.54	134.2 ± 18.38	0.0033
NLRP3 (ng/mL)	0.92 ± 0.13	2.95 ± 1.27	<0.0001
XOR (U/L)	19.21 ± 4.89	24.69 ± 10.68	0.0088
XO (U/L)	14.96 ± 4.00	16.33 ± 5.22	–
XO/XOR ratio	0.79 ± 0.15	0.77 ± 0.36	–
Hypertension	35.48%	0.8889	–
Diabetes	0%	0.2889	–

Systolic blood pressure (SBP), Diastolic blood pressure (DBP), estimated glomerular filtration rate (eGFR), Serum creatinine (Scr), Blood urea nitrogen (BUN), Uric acid (UA), Fasting blood glucose (FBG), Total protein (TP), Albumin (Alb), Alanine transaminase (ALT), Aspartate transaminase (AST), Total cholesterol (TC), Triglyceride (TG), Red blood cell (RBC), White blood cell (WBC), Platelet (PLT), Hemoglobin (Hb), NOD-like receptor thermal protein domain-associated protein 3 (NLRP3), Xanthine oxidoreductase (XOR), Xanthine oxidase (XO). Values indicated the mean ± SD, Nonparametric test was used for comparisons of all variables.

Screening for the key marker of CKD

We performed LASSO logistic regression algorithm and random forest algorithm to screen for molecular markers of CKD from differentially expressed genes. The best lambda was selected after cross-validation to build the final LASSO model (Figures 4A and 4B), and then, 29 genes were identified from DEGs as the molecular markers (Figure 4E). In addition, we used random forest algorithm to detect 21 genes based on 10-fold cross-validation (Figures 4C and 4D). Finally, XDH, kidney oxidase-1 (KOX-1), cytochrome *c* oxidase subunit 2 (COX-2), reactive oxygen species modulator 1 (ROMO1), nitric oxide-associated protein 1 (NOA1), and nuclear factor NF-κB (NF-κB) were obtained by overlapping these two algorithms (Figure 4E, left). Except COX-2, the expression levels of other five genes, namely, XDH, KOX-1, ROMO1, NOA1, and NF-κB, increased in the CKD group (Figure 4E, right). These genes included five upregulated genes and one downregulated gene (Figure 4E, right). Surprisingly, XDH, COX-2, NF-κB, and KOX-1 have been reported to affect the levels of UA.[31–34] Taken together, these data suggest that these six marker genes might be used to develop a prediction tool to classify the CKD and normal control samples.

Validation of six marker genes in the simulated models of kidney fibrosis

To further validate the expression of the six marker genes, the proximal tubular epithelial cells were treated with TGF-β to simulate models of kidney fibrosis. Compared with control groups, XDH, KOX-1, and

Table 2. Causes of CKD patients

Cause of CKD	Percentage
Chronic glomerulonephritis	65.56%
Renal vascular disease	14.44%
Diabetic nephropathy	8.88%
Polycystic kidney	6.67%
Unilateral renal atrophy	3.33%
Solitary kidney	1.11%

The percentage of CKD patients with different etiology (n = 90).

ROMO1 were significantly upregulated by TGF-β treatment (Figure 5); however, the expression levels of NOA1, NF-κB, and COX-2 did not significantly change after the treatment with TGF-β. Collectively, the results of qRT-PCR of XDH, KOX-1, and ROMO1 were in accordance with the results of bioinformatics analyses, indicating that these three genes might be candidate markers.

Profile of metabolomics in the models of kidney fibrosis induced by TGF-β

In the simulated models of kidney fibrosis, we performed metabolomics analysis to investigate whether the end product of XOR activity was involved in CKD (Figure 1C). Of 1542 metabolites, 471 metabolites were annotated by three standard databases, including BMDB (56), ChemSpider (350), and mzCloud (66) (Figure 6A and Table S3), and then the annotated metabolites were divided into four decreasing credibility levels, including level1, level2, level3, and level4 according to precursor ion, MS2 fragment spectra, and column retention time. As shown in Figure 6B, the credibility of the metabolites marked by level1 was higher than that of the metabolites marked by other three levels, while the number of the metabolites marked by level1 (32) was lower than that of the metabolites marked by other levels including level2 (52), level3 (38), and level4 (350) (Figure 6B). All annotated metabolites were also classified into four subclasses, including phytochemical compounds, lipids, compounds with biological roles, and others with identification information. The number of the metabolites classified as lipids (64), compounds with biological roles (18), and others (50) was significantly lower than that of the metabolites classified as phytochemical compounds (340), and phytochemical compounds were composed of six major categories (accounting about 41%), including amino acids, peptides, and analogs (39), benzene and derivatives (21), organic acids (17), carbohydrates (16), amines and derivatives (16), and purines and derivatives (14) (Figure 6C). KEGG pathway analysis indicated that the annotated metabolites were involved in the top 10 KEGG pathways, including amino acid metabolism (25), nucleotide metabolism (19), metabolism of cofactors and vitamins (16), lipid metabolism (15), xenobiotics biodegradation and metabolism (13), carbohydrate metabolism (13), energy metabolism (7), biosynthesis of other secondary metabolites (5), metabolism of other amino acids (2), and metabolism of terpenoids and polyketides (1) (Figure 6D).

Differentially expressed metabolites in the simulated models of kidney fibrosis *in vitro*

PCA of the metabolites indicated that five biological replicates of control and simulated models induced by TGF-β were highly correlated and clustered (Figure 7A). Based on the abundance of the annotated metabolites, 152 upregulated and 158 downregulated metabolites were identified (Figure 7B) with fold change >1.5 and p value <0.05. Consistent with previous findings that UA is commonly elevated in patients with CKD, our KEGG pathway enrichment analysis revealed that purine metabolism was also enriched in differentially expressed metabolites (Figure 7C). A striking example was xanthine, generated by XDH, which increased in TGF-β sample. The pathway network indicated that $\tilde{I}^2$—d—3—ribofuranosyluric acid (Figure 7D) was also related to purine metabolism. In summary, the profile of differentially expressed metabolites suggests that the products of metabolism related to XOR activity might influence CKD.

DISCUSSION

Although UA, the end product of XOR activity, is commonly elevated in subjects with CKD, the underlying relationship between XOR activity and CKD is still unclear. We analyzed clinical data, CKD datasets from the GEO database, and untargeted metabolomics to investigate the relationship between XOR activity and CKD (Figure 1).

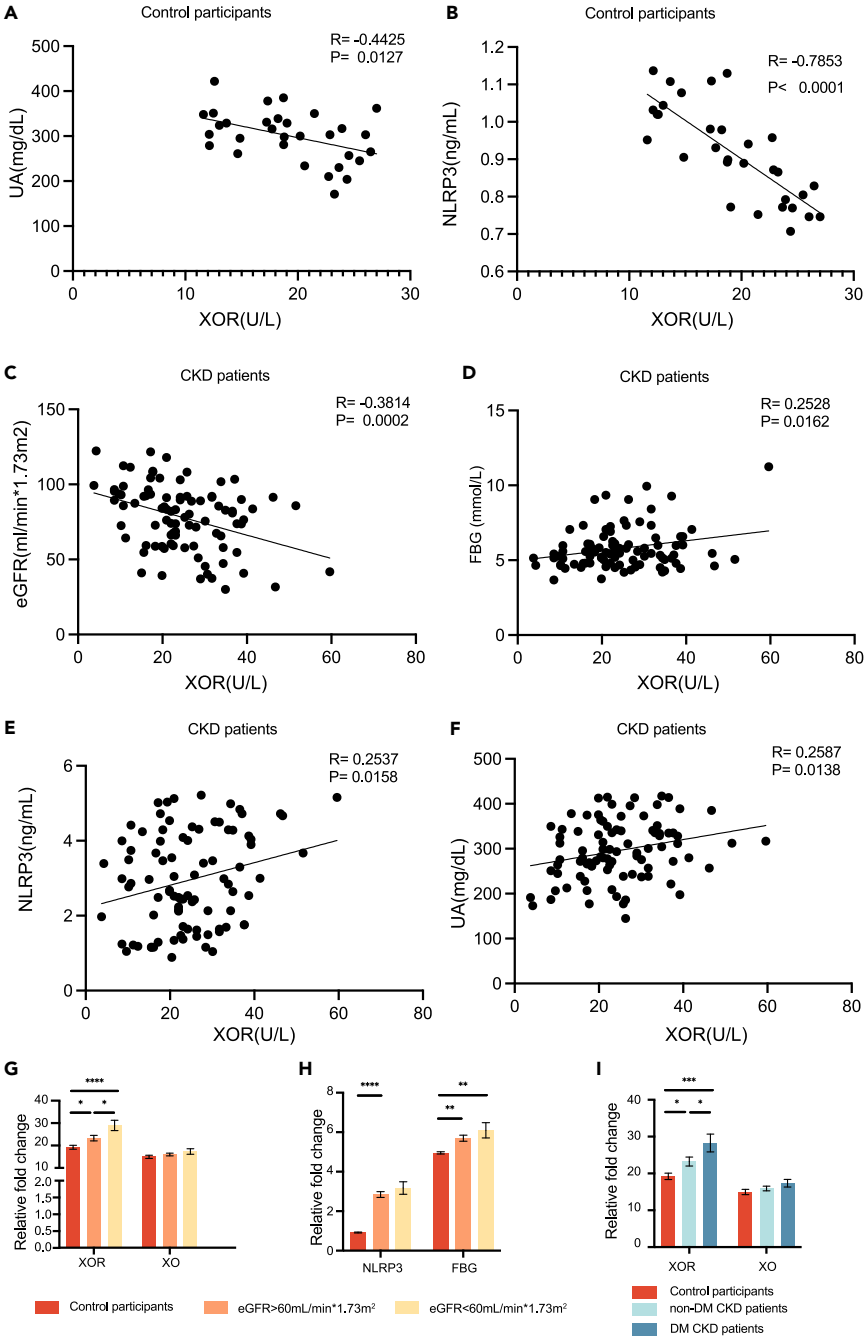

Figure 2. Systematic analysis of clinical data in this study

(A and B) Point plot showing that XOR was negatively correlated with UA(A) and NLRP3 (B) in the control group.

(C–F) Point plot showing the correlation between XOR and eGFR (C), FBG (D), NLRP3 (E), and UA (F).

(G and H) Bar plots showing the abundance of XOR, XO, XO/XOR ratio, NLRP3, and FBG into the control groups and two CKD groups according to the eGFR level, for the group with eGFR<60 mL/(min·1.73 m^2). *p < 0.05, **p < 0.01, ***p < 0.001, and ****p < 0.0001.

(I) Bar plot showing the abundance of XOR and XDH in control groups and the CKD patient groups, including DM and non-DM groups.

CKD is a progressive disease and its routine clinical assessment is based on measuring markers of kidney damage and estimating renal function. The kidney damage was evaluated by proteinuria, abnormalities of urine sediment, abnormalities of electrolytes induced by abnormalities of kidney tubules, and

A

GEO Accession ID	Platform	Number of Cases	Number of Controls	Tissue	paper
GSE15072	GPL570	9	8	peripheral blood	10.1371/journal.pone.0122272
GSE66494	GPL6480	54	8	renal biopsy	10.1371/journal.pone.0136994
GSE45980	GPL13497	43	-	renal biopsy	10.1111/eci.12585
GSE69438	GPL11670	6	-	renal biopsy	10.1126/scitranslmed.aac7071
GSE70528	GPL570	7	-	peripheral blood	10.1007/s10157-015-1150-y

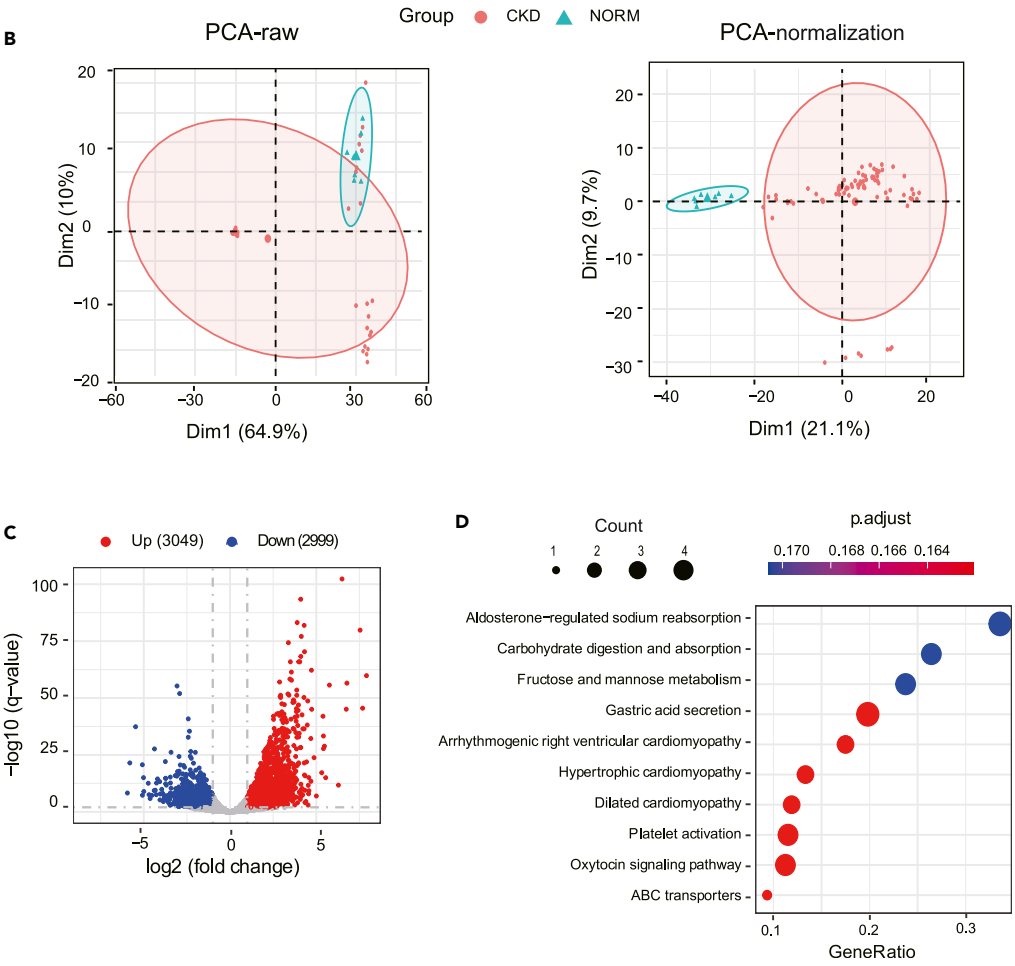

Figure 3. Screening the differentially expressed genes for CKD

(A) The detailed information of the five datasets including 119 CKD patients and 16 healthy subjects.

(B) Plot of principal component analysis (PCA) before and after sample correction. The red and blue colored blocks represent the groups of CKD and healthy subjects.

(C) Volcano plots of differentially expressed genes involved in CKD. Red and green points indicate up- and downregulation of genes, respectively, between CKD and healthy subjects.

(D) KEGG pathway enrichment analysis of differentially expressed genes. The top 10 KEGG categories are displayed.

abnormalities of histology, while eGFR using the Scr[20] and BUN[21–23] was considered an estimate of renal function. At the clinical level, we found that XOR activity correlated with previously reported physiological characteristics related to CKD, such as Scr, BUN, and eGFR (Figure 2 and Table S1); however, it is

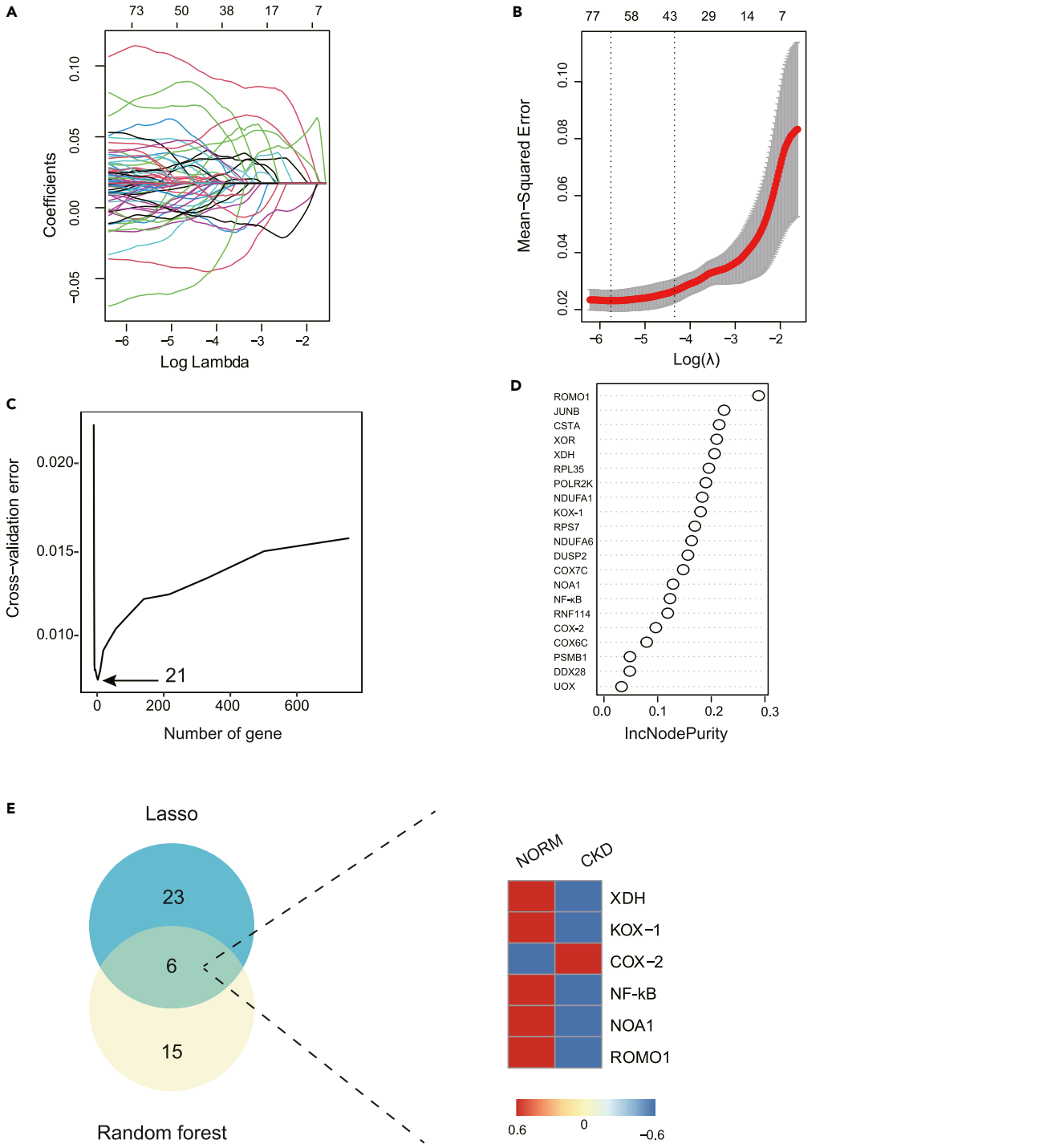

Figure 4. Hub genes selected by LASSO regression analysis and random forest in GEO datasets of CKD

(A) LASSO coefficient profiles of the hub CKD genes.

(B) Plot of mean squared error by lambda value.

(C) Plot of cross-validation error of random forest. The arrow indicates the number of important variables.

(D) Twenty-one important variables were ranked by IncNodePurity.

(E) Venn plot and heatmap plot showing the number (left) of overlapped genes between LASSO and random forest algorithms, and the abundance changes (right) of the overlapped genes (including XDH, KOX-1, COX-2, ROMO1, NOA1, and NF-κB).

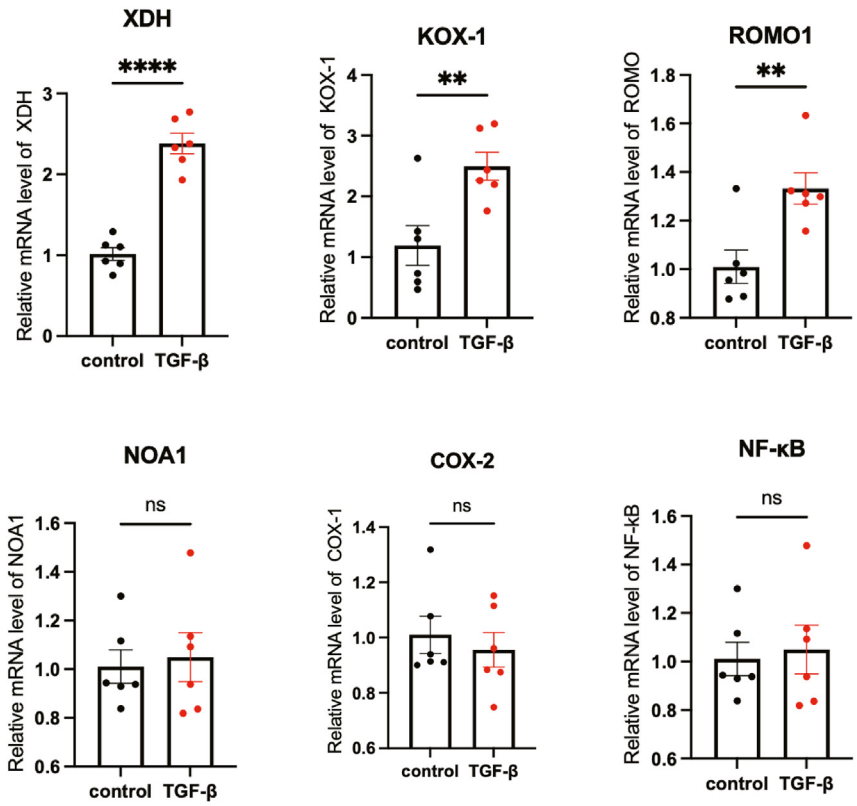

Figure 5. Comparison of gene expression levels of six marker genes between controls and TGF-β samples via qRT-PCR

The mRNA levels of XDH, KOX-1, ROMO1, NOA1, COX-2, and NF-κB were analyzed by qRT-PCR in TGF-β-treated HK2 cells and control cells. Differences were calculated using the $2^{-\Delta\Delta Ct}$ method by comparing gene expression levels to those in HK2 cells. All data were analyzed using the Student's *t* test. Asterisks and ns indicate significant and nonsignificant differences between the groups, respectively. n = 6, **p < 0.01, ****p < 0.0001.

interesting that the association of XOR with UA and NLRP3 in the physiological situation was opposite to that in CKD patients, which may be related to the oxidation and antioxidant effects of UA, which has a dynamic transformation process with XOR.[35] Further research on CKD patients grouped according to eGFR and whether or not they had diagnosis showed that the XOR level was affected by both FBG and eGFR. It has been demonstrated that the XO/XOR ratio reflects the conversion rate of XDH to XO.[36] The generation rate of ROS by XO in the human body is significantly higher than that by XDH. Hence, an increase in the XO/XOR ratio accelerates the generation of ROS.[37] This suggests that ROS production may be promoted by promoting the conversion of XDH to XO in the early stage of CKD to further damage the kidney. In summary, inhibition of XOR activity may delay the progression of CKD by suppressing NLRP3 and reducing FBG level. Specifically, inhibition of XOR activity had a more significant effect disease degree if eGFR<60 mL/(min·1.73 m^2). This conclusion indicates that similar to BUN and eGFR, XOR activity might also be a potential diagnostic maker in clinical context. Further investigation of how XOR activity regulates these processes will provide insight into the process of CKD.

Transcriptome analysis technologies are important systems-biology methods for comprehensive understanding of how genes are expressed and interconnected.[38,39] The machine learning approach has been reported as a complementary method to identify the critical genes for the disease and malignancy in a transcriptome dataset.[40] At the transcriptomic level, emerging studies have revealed that several known genes such as PKD1, COL4A5, PKD2, COL4A4, COL4A3, and TTR exhibit strong associations with CKD.[41] In this study, we performed LASSO logistic regression algorithm and random forest algorithm to screen for the molecular markers such as XDH, KOX-1, COX, ROMO1, NOA1, and NF-κB for classifying the CKD and normal control samples (Figure 3 and Table S2). In agreement with the results of bioinformatics analyses, XDH, KOX-1, and ROMO1 were also expressed in the models of CKD (Figure 5). Surprisingly, XDH, the

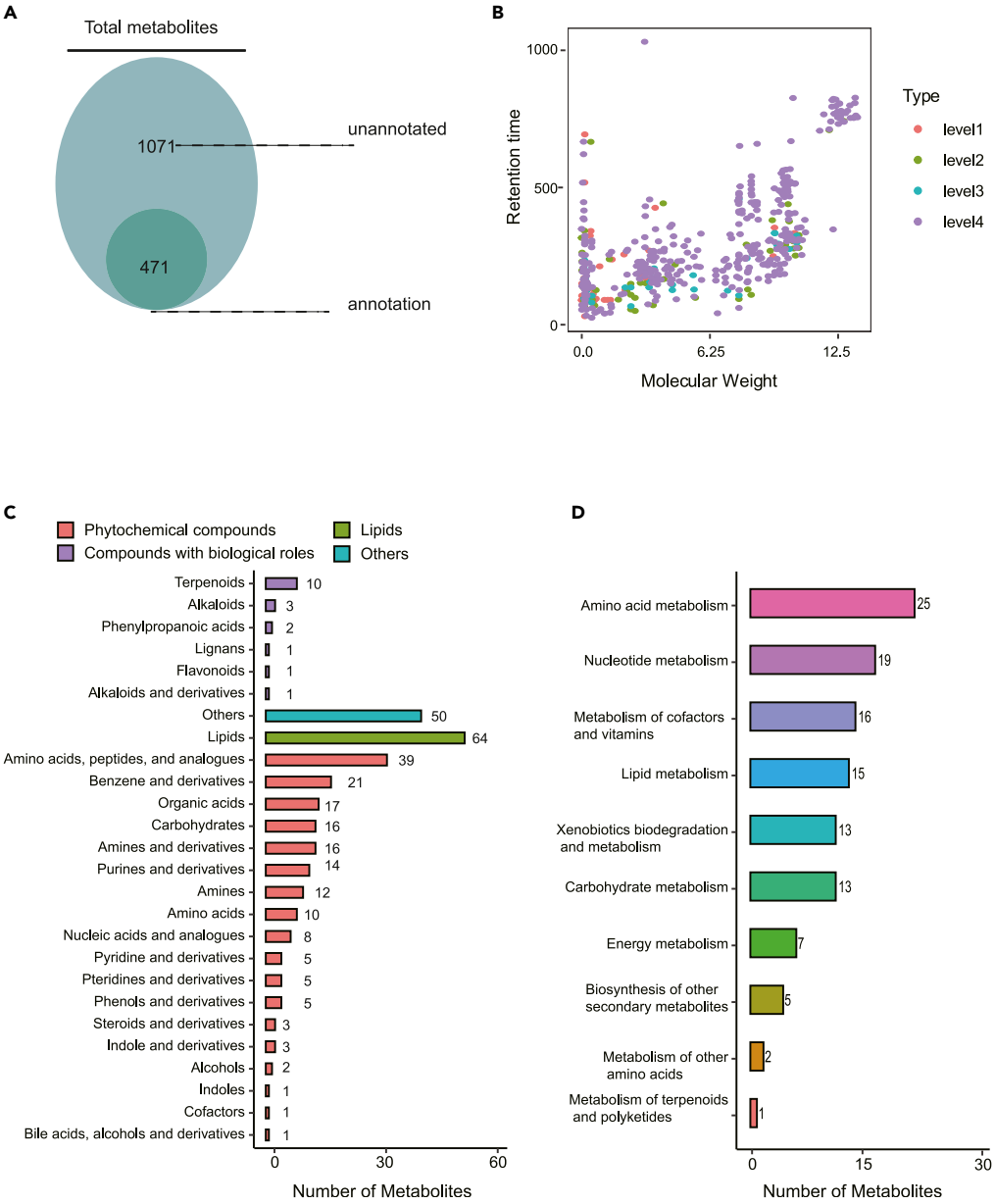

Figure 6. Summary of untargeted metabolomics datasets in this study

(A) Number of all identified metabolites (1542) and annotated metabolites (471).

(B) Molecular weight and retention time of annotated metabolites with four different credibility levels. Red, yellow, green, and purple indicate levels 1 to 4.

(C) Number of four subclasses including phytochemical compounds (340), lipids (64), compounds with biological roles (18), and others (50).

(D) The top 10 KEGG pathways of the annotated metabolites.

superoxide-producing form of XOR, is a critical enzyme in purine metabolism, which catalyzes oxidation of hypoxanthine to xanthine and oxidation of xanthine to UA.[31] Furthermore, KOX-1, which is generated superoxide by constituting NADPH oxidase, has been shown to play a crucial role in UA-induced oxidative stress and apoptosis in renal tubular cells.[34] ROMO1, a nuclear-encoded mitochondrial inner membrane protein that regulates mitochondrial ROS production,[42] is produced by XOR during the reaction process.[4,5] These results suggest that UA or ROS production generated by XOR activity involved in CKD processes might play an important role in the underlying molecular mechanism.

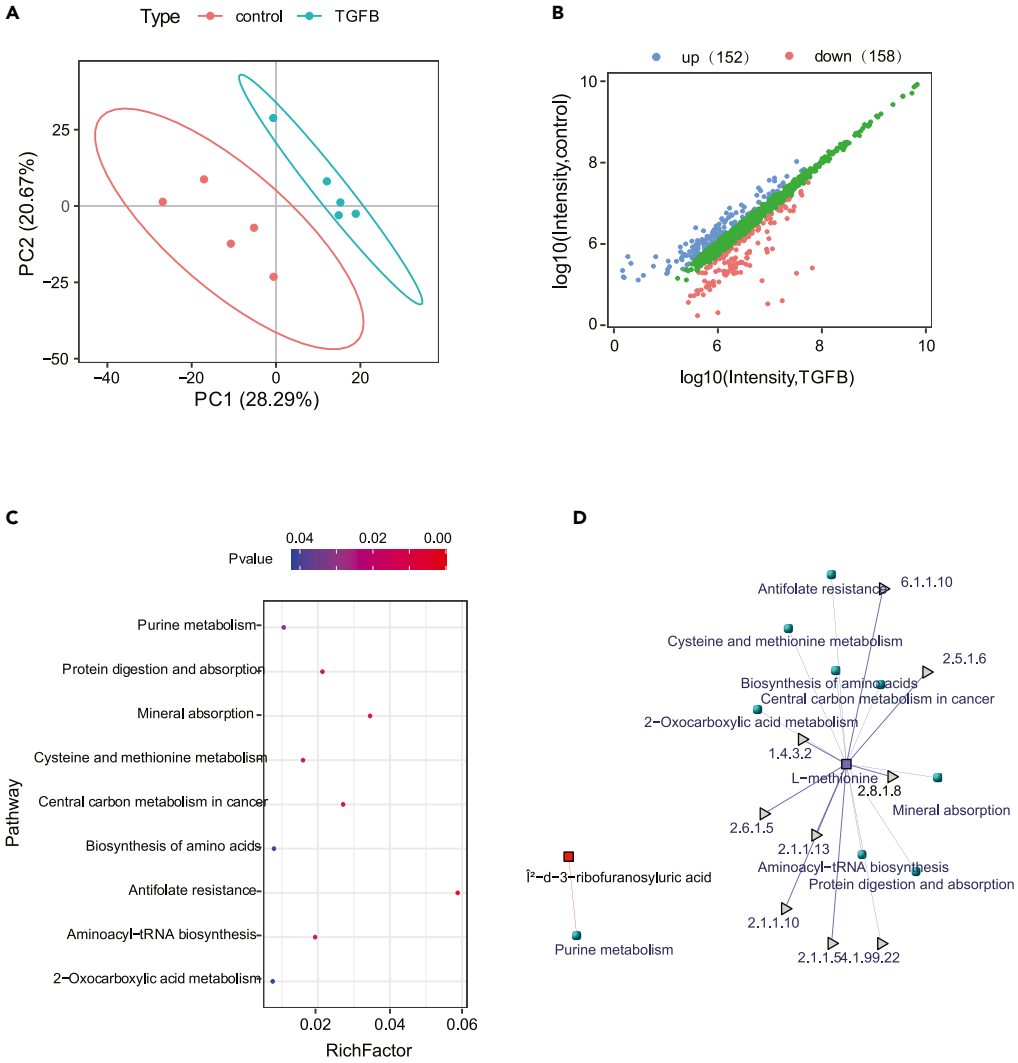

Figure 7. Differential metabolites induced by TGF-β

(A) Principal component analysis (PCA) of the metabolites of five biological replicates of control and TGF-β. Red and green points indicate the group of control group and TGF-β groups, respectively.

(B) The scatterplot shows the differential levels of metabolites in response to TGF-β. Red and green points indicate up- and downregulated metabolites, respectively, between the control and TGF-β groups.

(C) The point plot shows the KEGG pathways enriched for TGF-β-induced metabolites.

(D) Correlation network diagram of differential metabolites and KEGG pathways. The circle, triangle and square indicate the pathway, enzyme, and metabolites, respectively.

Metabolomics directly reflects the outcome of complex networks of biochemical reactions and provides insights into multiple aspects of cellular physiology by generating and integrating the profile of small metabolites, which originate from cellular metabolism.[43] Metabolomics has also been instrumental for the identification of new biomarkers of CKD.[44] An obvious example is 5-methoxytryptophan, whose levels strongly correlate with clinical markers of kidney disease by using untargeted metabolomics.[45] In our study, we identified 1543 metabolites by using untargeted metabolomics, and 472 metabolites were annotated by three standard databases (Figure 6A and Table S3). Of 152 upregulated and 158 downregulated metabolites, xanthine generated by XDH was upregulated by TGF-β, and purine metabolism was also enriched in the differentially expressed metabolites as shown in KEGG pathway enrichment analysis (Figure 7C, Table S3), which is consistent with the previous finding that UA is commonly elevated in CKD patients.[46]

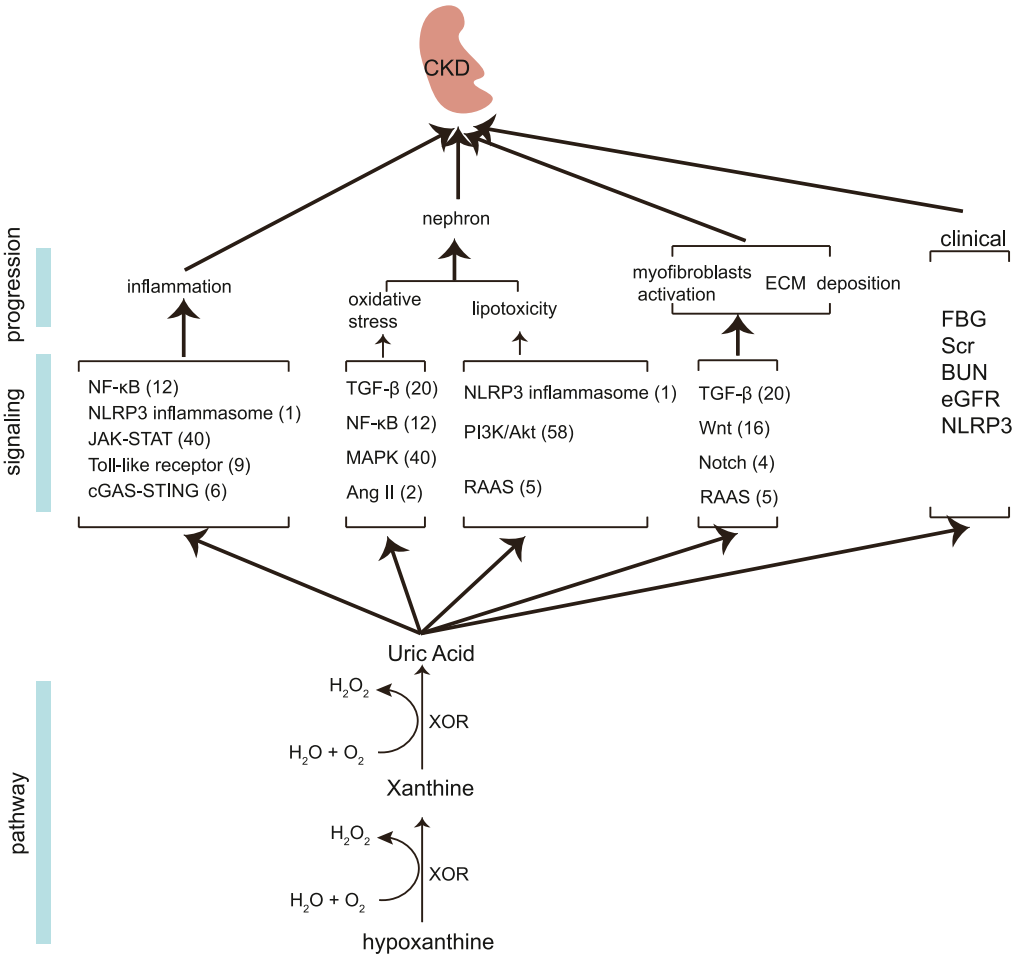

Figure 8. Summary relationship between XOR activity and CKD

Several key signaling pathways, such as NLRP3 inflammasome signaling, TGF-β signaling, and RAAS signaling, have been reported to affect the core characteristics of CKD, including nephron loss, inflammation, myofibroblasts activation, and extracellular matrix (ECM) deposition and are all modulated by the UA.

To further investigate the detailed correlation between XOR activity and CKD, we have summarized the multi-omics dataset based on the previous finding in a schematic for CKD and XOR in Figure 8. Nephron loss, inflammation, myofibroblasts activation, and extracellular matrix (ECM) deposition are the main processes of the initiation and progression of CKD.[47–49] It has been shown that the loss of tubules, glomeruli, and endothelium is promoted by lipotoxicity and oxidative stress,[50] which is modulated by the signaling of NLRP3 inflammasome,[51] , PI3K/Akt,[52] RAAS[53] or TGF-β,[54–56] NF-κB,[57–59] MAPK,[60] and Ang II.[61,62] The major signaling pathways that mediate inflammation have been found to be associated with these signaling of NF-κB,[63–65] NLRP3 inflammasome,[66,67] JAK-STAT,[68–71] Toll-like receptor,[72–74] and cGAS-STING[75–77] signaling. TGF-β signaling,[78,79] Wnt signaling,[80–85] RAAS signaling,[86,87] and Notch signaling[88–90] have been linked to the activation of myofibroblasts and the generation of ECM. This view was also supported by two major lines of evidence in our study. One is that several genes from these signaling pathways showed different expression between CKD patients and healthy subjects (Figure 8 and Table S4). For instance, of 12 identified genes in NF-κB signaling, 8 and 4 genes showed significantly increasing or decreasing level in CKD groups, respectively (Table S4). Other evidence is that five molecular markers such as KOX-1, ROMO1, COX-2, NOA1, and NF-κB except for XDH, generated from machine learning for classifying the CKD and normal control samples, were also reported to be associated with UA-oxidative stress.[34,64,91,92] Interestingly, UA, produced from xanthine and catalyzed by XDH,[31] has been proven to induce inflammation, oxidative stress, and activation of myofibroblasts.[93] Furthermore, XOR activity is an oxidative stress indicator for the need for renal replacement therapy and is

associated with the severity of CKD in a general Japanese population.[94,95] These results indicated that XOR activity might contribute to predict CKD.

Limitations of the study

The main limitations to our study are as follows: 1) there were a small number of clinical participants; 2) the analysis of the metabolomics level from the CKD group remained unknown and the underlying molecular mechanism by which XOR activity affects the process of CKD remained unclear. Thus, further investigation is needed to confirm our findings by obtaining metabolomics from CKD group and more clinical data.

In summary, these results suggest that the activity of XOR, the critical enzyme in purine metabolism, might be involved in the process of CKD by generating xanthine. Our results highlight the potential interplay between XOR activity and CKD in three aspects, including clinical, transcriptomic, and metabolomics levels.

STAR★METHODS

Detailed methods are provided in the online version of this paper and include the following:

- KEY RESOURCES TABLE
- RESOURCE AVAILABILITY
  - Lead contact
  - Material availability
  - Data and code availability
- EXPERIMENTAL MODEL AND STUDY PARTICIPANT DETAILS
  - Human participants
  - Ethical approval
  - Consent for publication
  - Cell
- METHOD DETAILS
  - Plasma XOR activity
  - Sample selection, data acquisition, and processing
  - Identification of hub CKD genes
  - Constructing samples induced by TGFβ
  - Quantitative real-time PCR (qRT-PCR)
  - Metabolite extraction, UPLC-MS analysis, and metabolite identification
  - Data preprocessing, quality control, and screening for the differential metabolites
- QUANTIFICATION AND STATISTICAL ANALYSIS
  - Statistical analysis

SUPPLEMENTAL INFORMATION

Supplemental information can be found online at https://doi.org/10.1016/j.isci.2023.107332.

ACKNOWLEDGMENTS

This study was supported by grants from the National Natural Science Foundation of China (82170757), and the Postgraduate Research and Practice Innovation Program of Jiangsu Province of China (Grant Number: KYCX21_2702). We are grateful to all participants, and we thank LetPub (www.letpub.com) for linguistic assistance and pre-submission expert review.

AUTHOR CONTRIBUTIONS

Y.Z. conceived of the study and participated in its design with drafting the manuscript. X.D. participated in the design of the study and performed the statistical analysis. L.G. participated in the sequence alignment. Y.Z. carried out the molecular genetic studies, J.X. performed the statistical analysis. Y.X. participated in its design, coordination, and the sequence alignment. H.L. conceived of the study and helped to draft the manuscript. D.Z. conceived of the study and participated in its design and coordination and helped to draft the manuscript, D.Z. responsible for all data, figures, and text. All authors read and approved the final manuscript.

DECLARATION OF INTERESTS

The authors declare that they have no competing interests.

INCLUSION AND DIVERSITY

We support inclusive, diverse, and equitable conduct of research.

Received: March 1, 2023
Revised: May 19, 2023
Accepted: July 5, 2023
Published: July 10, 2023

REFERENCES

1. Battelli, M.G., Bolognesi, A., and Polito, L. (2014). Pathophysiology of circulating xanthine oxidoreductase: new emerging roles for a multi-tasking enzyme. Biochim. Biophys. Acta *1842*, 1502–1517. https://doi.org/10.1016/j.bbadis.2014.05.022.

2. Kusano, T., Nishino, T., Okamoto, K., Hille, R., and Nishino, T. (2023). The mechanism and significance of the conversion of xanthine dehydrogenase to xanthine oxidase in mammalian secretory gland cells. Redox Biol. *59*, 102573. https://doi.org/10.1016/j.redox.2022.102573.

3. Cantu-Medellin, N., and Kelley, E.E. (2013). Xanthine oxidoreductase-catalyzed reactive species generation: A process in critical need of reevaluation. Redox Biol. *1*, 353–358. https://doi.org/10.1016/j.redox.2013.05.002.

4. Ishii, T., Taguri, M., Tamura, K., and Oyama, K. (2017). Evaluation of the Effectiveness of Xanthine Oxidoreductase Inhibitors on Haemodialysis Patients using a Marginal Structural Model. Sci. Rep. *7*, 14004. https://doi.org/10.1038/s41598-017-13970-4.

5. Kelley, E.E. (2015). A new paradigm for XOR-catalyzed reactive species generation in the endothelium. Pharmacol. Rep. *67*, 669–674. https://doi.org/10.1016/j.pharep.2015.05.004.

6. Rysz, J., Gluba-Brzózka, A., Franczyk, B., Jabłonowski, Z., and Ciałkowska-Rysz, A. (2017). Novel Biomarkers in the Diagnosis of Chronic Kidney Disease and the Prediction of Its Outcome. Int. J. Mol. Sci. *18*, 1702. https://doi.org/10.3390/ijms18081702.

7. Senanayake, S., Gunawardena, N., Palihawadana, P., Kularatna, S., and Peiris, T.S.G. (2017). Validity and reliability of the Sri Lankan version of the kidney disease quality of life questionnaire (KDQOL-SF). Health Qual. Life Outcomes *15*, 119. https://doi.org/10.1186/s12955-017-0697-6.

8. Hill, N.R., Fatoba, S.T., Oke, J.L., Hirst, J.A., O'Callaghan, C.A., Lasserson, D.S., and Hobbs, F.D.R. (2016). Global Prevalence of Chronic Kidney Disease - A Systematic Review and Meta-Analysis. PLoS One *11*, e0158765. https://doi.org/10.1371/journal.pone.0158765.

9. Lu, J.L., Molnar, M.Z., Naseer, A., Mikkelsen, M.K., Kalantar-Zadeh, K., and Kovesdy, C.P. (2015). Association of age and BMI with kidney function and mortality: a cohort study. Lancet Diabetes Endocrinol. *3*, 704–714. https://doi.org/10.1016/S2213-8587(15)00128-X.

10. Tonneijck, L., Muskiet, M.H.A., Smits, M.M., van Bommel, E.J., Heerspink, H.J.L., van Raalte, D.H., and Joles, J.A. (2017). Glomerular Hyperfiltration in Diabetes: Mechanisms, Clinical Significance, and Treatment. J. Am. Soc. Nephrol. *28*, 1023–1039. https://doi.org/10.1681/ASN.2016060666.

11. Thomas, B., Matsushita, K., Abate, K.H., Al-Aly, Z., Ärnlöv, J., Asayama, K., Atkins, R., Badawi, A., Ballew, S.H., Banerjee, A., et al. (2017). Global Cardiovascular and Renal Outcomes of Reduced GFR. J. Am. Soc. Nephrol. *28*, 2167–2179. https://doi.org/10.1681/ASN.2016050562.

12. Vivante, A., and Hildebrandt, F. (2016). Exploring the genetic basis of early-onset chronic kidney disease. Nat. Rev. Nephrol. *12*, 133–146. https://doi.org/10.1038/nrneph.2015.205.

13. Uy, N., and Reidy, K. (2016). Developmental Genetics and Congenital Anomalies of the Kidney and Urinary Tract. J. Pediatr. Genet. *5*, 51–60. https://doi.org/10.1055/s-0035-1558423.

14. Glaser, J., Lemery, J., Rajagopalan, B., Diaz, H.F., García-Trabanino, R., Taduri, G., Madero, M., Amarasinghe, M., Abraham, G., Anutrakulchai, S., et al. (2016). Climate Change and the Emergent Epidemic of CKD from Heat Stress in Rural Communities: The Case for Heat Stress Nephropathy. Clin. J. Am. Soc. Nephrol. *11*, 1472–1483. https://doi.org/10.2215/CJN.13841215.

15. Andersen, K., Kesper, M.S., Marschner, J.A., Konrad, L., Ryu, M., Kumar Vr, S., Kulkarni, O.P., Mulay, S.R., Romoli, S., Demleitner, J., et al. (2017). Intestinal Dysbiosis, Barrier Dysfunction, and Bacterial Translocation Account for CKD-Related Systemic Inflammation. J. Am. Soc. Nephrol. *28*, 76–83. https://doi.org/10.1681/ASN.2015111285.

16. Kidney Disease Improving Global Outcomes KDIGO Glomerular Diseases Work Group (2021). KDIGO 2021 Clinical Practice Guideline for the Management of Glomerular Diseases. Kidney Int. *100*, S1–S276. https://doi.org/10.1016/j.kint.2021.05.021.

17. Alassar, A., Roy, D., Abdulkareem, N., Valencia, O., Brecker, S., and Jahangiri, M. (2012). Acute kidney injury after transcatheter aortic valve implantation: incidence, risk factors, and prognostic effects. Innovations *7*, 389–393. https://doi.org/10.1177/155698451200700603.

18. Mirzaee, M., Jamee, M., Mohkam, M., Abdollah Gorji, F., Khalili, M., Rafiei Tabatabaei, S., Karimi, A., Armin, S., Mansour Ghanaie, R., Fahimzad, S.A., et al. (2023). Acute Kidney Injury in Pediatric Patients with COVID-19; Clinical Features and Outcome. Iran. J. Kidney Dis. *1*, 20–27.

19. Hirano, D., Ishikura, K., Uemura, O., Ito, S., Wada, N., Hattori, M., Ohashi, Y., Hamasaki, Y., Tanaka, R., Nakanishi, K., et al. (2016). Association between low birth weight and childhood-onset chronic kidney disease in Japan: a combined analysis of a nationwide survey for paediatric chronic kidney disease and the National Vital Statistics Report. Nephrol. Dial. Transplant. *31*, 1895–1900. https://doi.org/10.1093/ndt/gfv425.

20. Romagnani, P., Remuzzi, G., Glassock, R., Levin, A., Jager, K.J., Tonelli, M., Massy, Z., Wanner, C., and Anders, H.J. (2017). Chronic kidney disease. Nat. Rev. Dis. Primers *3*, 17088. https://doi.org/10.1038/nrdp.2017.88.

21. Arif, H., Khatri, M., and Kumar, S. (2022). What are the factors affecting the progression of kidney failure mortality and morbidity after cardiac surgery in patients with chronic kidney disease? J. Card. Surg. *37*, 2495–2496. https://doi.org/10.1111/jocs.16539.

22. Kim, H.J., Kim, T.E., Han, M., Yi, Y., Jeong, J.C., Chin, H.J., Song, S.H., Lee, J., Lee, K.B., Sung, S., et al. (2021). Effects of blood urea nitrogen independent of the estimated glomerular filtration rate on the development of anemia in non-dialysis chronic kidney disease: The results of the KNOW-CKD study. PLoS One *16*, e0257305. https://doi.org/10.1371/journal.pone.0257305.

23. Seki, M., Nakayama, M., Sakoh, T., Yoshitomi, R., Fukui, A., Katafuchi, E., Tsuda, S., Nakano, T., Tsuruya, K., and Kitazono, T. (2019). Blood urea nitrogen is

independently associated with renal outcomes in Japanese patients with stage 3-5 chronic kidney disease: a prospective observational study. BMC Nephrol. *20*, 115. https://doi.org/10.1186/s12882-019-1306-1.

24. Kirkman, D.L., Muth, B.J., Ramick, M.G., Townsend, R.R., and Edwards, D.G. (2018). Role of mitochondria-derived reactive oxygen species in microvascular dysfunction in chronic kidney disease. Am. J. Physiol. Renal Physiol. *314*, F423–F429. https://doi.org/10.1152/ajprenal.00321.2017.

25. Sureshbabu, A., Ryter, S.W., and Choi, M.E. (2015). Oxidative stress and autophagy: crucial modulators of kidney injury. Redox Biol. *4*, 208–214. https://doi.org/10.1016/j.redox.2015.01.001.

26. Locatelli, F., Canaud, B., Eckardt, K.U., Stenvinkel, P., Wanner, C., and Zoccali, C. (2003). Oxidative stress in end-stage renal disease: an emerging threat to patient outcome. Nephrol. Dial. Transplant. *18*, 1272–1280. https://doi.org/10.1093/ndt/gfg074.

27. Hambali, Z., Ahmad, Z., Arab, S., and Khazaai, H. (2011). Oxidative stress and its association with cardiovascular disease in chronic renal failure patients. Indian J. Nephrol. *21*, 21–25. https://doi.org/10.4103/0971-4065.75218.

28. Popolo, A., Autore, G., Pinto, A., and Marzocco, S. (2013). Oxidative stress in patients with cardiovascular disease and chronic renal failure. Free Radic. Res. *47*, 346–356. https://doi.org/10.3109/10715762.2013.779373.

29. Houston, M., Estevez, A., Chumley, P., Aslan, M., Marklund, S., Parks, D.A., and Freeman, B.A. (1999). Binding of xanthine oxidase to vascular endothelium. Kinetic characterization and oxidative impairment of nitric oxide-dependent signaling. J. Biol. Chem. *274*, 4985–4994. https://doi.org/10.1074/jbc.274.8.4985.

30. Nakatani, S., Ishimura, E., Murase, T., Nakamura, T., Nakatani, A., Toi, N., Nishide, K., Uedono, H., Tsuda, A., Kurajoh, M., et al. (2021). Plasma Xanthine Oxidoreductase Activity Associated with Glycemic Control in Patients with Pre-Dialysis Chronic Kidney Disease. Kidney Blood Press. Res. *46*, 475–483. https://doi.org/10.1159/000516610.

31. Yamaguchi, Y., Matsumura, T., Ichida, K., Okamoto, K., and Nishino, T. (2007). Human xanthine oxidase changes its substrate specificity to aldehyde oxidase type upon mutation of amino acid residues in the active site: roles of active site residues in binding and activation of purine substrate. J. Biochem. *141*, 513–524. https://doi.org/10.1093/jb/mvm053.

32. Oğuz, N., Kırça, M., Çetin, A., and Yeşilkaya, A. (2017). Effect of uric acid on inflammatory COX-2 and ROS pathways in vascular smooth muscle cells. J. Recept. Signal Transduct. Res. *37*, 500–505. https://doi.org/10.1080/10799893.2017.1360350.

33. Chen, Y., Xu, W., Chen, Y., Han, A., Song, J., Zhou, X., and Song, W. (2022). Renal NF-kappaB activation impairs uric acid homeostasis to promote tumor-associated mortality independent of wasting. Immunity *55*, 1594–1608.e6. https://doi.org/10.1016/j.immuni.2022.07.022.

34. Li, Z., Sheng, Y., Liu, C., Li, K., Huang, X., Huang, J., and Xu, K. (2016). Nox4 has a crucial role in uric acid-induced oxidative stress and apoptosis in renal tubular cells. Mol. Med. Rep. *13*, 4343–4348. https://doi.org/10.3892/mmr.2016.5083.

35. Liu, N., Xu, H., Sun, Q., Yu, X., Chen, W., Wei, H., Jiang, J., Xu, Y., and Lu, W. (2021). The Role of Oxidative Stress in Hyperuricemia and Xanthine Oxidoreductase (XOR) Inhibitors. Oxid. Med. Cell. Longev. *2021*, 1470380. https://doi.org/10.1155/2021/1470380.

36. Terawaki, H., Murase, T., Nakajima, A., Aoyagi, K., Fukushima, N., Tani, Y., Nakamura, T., and Kazama, J.J. (2017). The relationship between xanthine oxidoreductase and xanthine oxidase activities in plasma and kidney dysfunction. J. Clin. Exp. Nephrol. *02*, 31.

37. Terawaki, H., Hayashi, T., Murase, T., Iijima, R., Waki, K., Tani, Y., Nakamura, T., Yoshimura, K., Uchida, S., and Kazama, J.J. (2018). Relationship between Xanthine Oxidoreductase Redox and Oxidative Stress among Chronic Kidney Disease Patients. Oxid. Med. Cell. Longev. *2018*, 9714710. https://doi.org/10.1155/2018/9714710.

38. Stahl, F., Hitzmann, B., Mutz, K., Landgrebe, D., Lübbecke, M., Kasper, C., Walter, J., and Scheper, T. (2012). Transcriptome analysis. Adv. Biochem. Eng. Biotechnol. *127*, 1–25. https://doi.org/10.1007/10_2011_102.

39. Mutz, K.O., Heilkenbrinker, A., Lönne, M., Walter, J.G., and Stahl, F. (2013). Transcriptome analysis using next-generation sequencing. Curr. Opin. Biotechnol. *24*, 22–30. https://doi.org/10.1016/j.copbio.2012.09.004.

40. Aromolaran, O., Aromolaran, D., Isewon, I., and Oyelade, J. (2021). Machine learning approach to gene essentiality prediction: a review. Brief. Bioinform. *22*, bbab128. https://doi.org/10.1093/bib/bbab128.

41. Stelzer, G., Rosen, N., Plaschkes, I., Zimmerman, S., Twik, M., Fishilevich, S., Stein, T.I., Nudel, R., Lieder, I., Mazor, Y., et al. (2016). The GeneCards Suite: From Gene Data Mining to Disease Genome Sequence Analyses. Curr. Protoc. Bioinformatics *54*. 1.30.1 30 1.30.33-31 30 33. https://doi.org/10.1002/cpbi.5.

42. Na, A.R., Chung, Y.M., Lee, S.B., Park, S.H., Lee, M.S., and Yoo, Y.D. (2008). A critical role for Romo1-derived ROS in cell proliferation. Biochem. Biophys. Res. Commun. *369*, 672–678. https://doi.org/10.1016/j.bbrc.2008.02.098.

43. Liu, X., and Locasale, J.W. (2017). Metabolomics: A Primer. Trends Biochem. Sci. *42*, 274–284. https://doi.org/10.1016/j.tibs.2017.01.004.

44. Hocher, B., and Adamski, J. (2017). Metabolomics for clinical use and research in chronic kidney disease. Nat. Rev. Nephrol. *13*, 269–284. https://doi.org/10.1038/nrneph.2017.30.

45. Chen, D.Q., Cao, G., Chen, H., Argyopoulos, C.P., Yu, H., Su, W., Chen, L., Samuels, D.C., Zhuang, S., Bayliss, G.P., et al. (2019). Identification of serum metabolites associating with chronic kidney disease progression and anti-fibrotic effect of 5-methoxytryptophan. Nat. Commun. *10*, 1476. https://doi.org/10.1038/s41467-019-09329-0.

46. Kosugi, T., Nakayama, T., Heinig, M., Zhang, L., Yuzawa, Y., Sanchez-Lozada, L.G., Roncal, C., Johnson, R.J., and Nakagawa, T. (2009). Effect of lowering uric acid on renal disease in the type 2 diabetic db/db mice. Am. J. Physiol. Renal Physiol. *297*, F481–F488. https://doi.org/10.1152/ajprenal.00092.2009.

47. Liu, Y. (2011). Cellular and molecular mechanisms of renal fibrosis. Nat. Rev. Nephrol. *7*, 684–696. https://doi.org/10.1038/nrneph.2011.149.

48. Zhou, D., and Liu, Y. (2016). Renal fibrosis in 2015: Understanding the mechanisms of kidney fibrosis. Nat. Rev. Nephrol. *12*, 68–70. https://doi.org/10.1038/nrneph.2015.215.

49. Humphreys, B.D. (2018). Mechanisms of Renal Fibrosis. Annu. Rev. Physiol. *80*, 309–326. https://doi.org/10.1146/annurev-physiol-022516-034227.

50. Jang, H.S., Noh, M.R., Kim, J., and Padanilam, B.J. (2020). Defective Mitochondrial Fatty Acid Oxidation and Lipotoxicity in Kidney Diseases. Front. Med. *7*, 65. https://doi.org/10.3389/fmed.2020.00065.

51. Meng, X.M. (2019). Inflammatory Mediators and Renal Fibrosis. Adv. Exp. Med. Biol. *1165*, 381–406. https://doi.org/10.1007/978-981-13-8871-2_18.

52. Bussolati, B., Deregibus, M.C., Fonsato, V., Doublier, S., Spatola, T., Procida, S., Di Carlo, F., and Camussi, G. (2005). Statins prevent oxidized LDL-induced injury of glomerular podocytes by activating the phosphatidylinositol 3-kinase/AKT-signaling pathway. J. Am. Soc. Nephrol. *16*, 1936–1947. https://doi.org/10.1681/ASN.2004080629.

53. Miller, E.R., 3rd, Juraschek, S.P., Anderson, C.A., Guallar, E., Henoch-Ryugo, K., Charleston, J., Turban, S., Bennett, M.R., and Appel, L.J. (2013). The effects of n-3 long-chain polyunsaturated fatty acid supplementation on biomarkers of kidney injury in adults with diabetes: results of the GO-FISH trial. Diabetes Care *36*, 1462–1469. https://doi.org/10.2337/dc12-1940.

54. Yan, X., and Chen, Y.G. (2011). Smad7: not only a regulator, but also a cross-talk mediator of TGF-beta signalling. Biochem.

J. *434*, 1–10. https://doi.org/10.1042/BJ20101827.

55. Das, R., Xu, S., Quan, X., Nguyen, T.T., Kong, I.D., Chung, C.H., Lee, E.Y., Cha, S.K., and Park, K.S. (2014). Upregulation of mitochondrial Nox4 mediates TGF-beta-induced apoptosis in cultured mouse podocytes. Am. J. Physiol. Renal Physiol. *306*, F155–F167. https://doi.org/10.1152/ajprenal.00438.2013.

56. Zhou, B., Mu, J., Gong, Y., Lu, C., Zhao, Y., He, T., and Qin, Z. (2017). Brd4 inhibition attenuates unilateral ureteral obstruction-induced fibrosis by blocking TGF-beta-mediated Nox4 expression. Redox Biol. *11*, 390–402. https://doi.org/10.1016/j.redox.2016.12.031.

57. Morgan, M.J., and Liu, Z.G. (2011). Crosstalk of reactive oxygen species and NF-kappaB signaling. Cell Res. *21*, 103–115. https://doi.org/10.1038/cr.2010.178.

58. Nlandu Khodo, S., Dizin, E., Sossauer, G., Szanto, I., Martin, P.Y., Feraille, E., Krause, K.H., and de Seigneux, S. (2012). NADPH-oxidase 4 protects against kidney fibrosis during chronic renal injury. J. Am. Soc. Nephrol. *23*, 1967–1976. https://doi.org/10.1681/ASN.2012040373.

59. Sedeek, M., Nasrallah, R., Touyz, R.M., and Hébert, R.L. (2013). NADPH oxidases, reactive oxygen species, and the kidney: friend and foe. J. Am. Soc. Nephrol. *24*, 1512–1518. https://doi.org/10.1681/ASN.2012111112.

60. Liles, J.T., Corkey, B.K., Notte, G.T., Budas, G.R., Lansdon, E.B., Hinojosa-Kirschenbaum, F., Badal, S.S., Lee, M., Schultz, B.E., Wise, S., et al. (2018). ASK1 contributes to fibrosis and dysfunction in models of kidney disease. J. Clin. Invest. *128*, 4485–4500. https://doi.org/10.1172/JCI99768.

61. Gorin, Y., Ricono, J.M., Kim, N.H., Bhandari, B., Choudhury, G.G., and Abboud, H.E. (2003). Nox4 mediates angiotensin II-induced activation of Akt/protein kinase B in mesangial cells. Am. J. Physiol. Renal Physiol. *285*, F219–F229. https://doi.org/10.1152/ajprenal.00414.2002.

62. Yang, Q., Wu, F.R., Wang, J.N., Gao, L., Jiang, L., Li, H.D., Ma, Q., Liu, X.Q., Wei, B., Zhou, L., et al. (2018). Nox4 in renal diseases: An update. Free Radic. Biol. Med. *124*, 466–472. https://doi.org/10.1016/j.freeradbiomed.2018.06.042.

63. Sanz, A.B., Sanchez-Niño, M.D., Ramos, A.M., Moreno, J.A., Santamaria, B., Ruiz-Ortega, M., Egido, J., and Ortiz, A. (2010). NF-kappaB in renal inflammation. J. Am. Soc. Nephrol. *21*, 1254–1262. https://doi.org/10.1681/ASN.2010020218.

64. Zhang, H., and Sun, S.C. (2015). NF-kappaB in inflammation and renal diseases. Cell Biosci. *5*, 63. https://doi.org/10.1186/s13578-015-0056-4.

65. Song, N., Thaiss, F., and Guo, L. (2019). NFkappaB and Kidney Injury. Front. Immunol. *10*, 815. https://doi.org/10.3389/fimmu.2019.00815.

66. Ding, H., Li, J., Li, Y., Yang, M., Nie, S., Zhou, M., Zhou, Z., Yang, X., Liu, Y., and Hou, F.F. (2021). MicroRNA-10 negatively regulates inflammation in diabetic kidney via targeting activation of the NLRP3 inflammasome. Mol. Ther. *29*, 2308–2320. https://doi.org/10.1016/j.ymthe.2021.03.012.

67. Xiong, W., Meng, X.F., and Zhang, C. (2021). NLRP3 Inflammasome in Metabolic-Associated Kidney Diseases: An Update. Front. Immunol. *12*, 714340. https://doi.org/10.3389/fimmu.2021.714340.

68. Brosius, F.C., 3rd, and He, J.C. (2015). JAK inhibition and progressive kidney disease. Curr. Opin. Nephrol. Hypertens. *24*, 88–95. https://doi.org/10.1097/MNH.0000000000000079.

69. Fragiadaki, M., Lannoy, M., Themanns, M., Maurer, B., Leonhard, W.N., Peters, D.J.M., Moriggl, R., and Ong, A.C.M. (2017). STAT5 drives abnormal proliferation in autosomal dominant polycystic kidney disease. Kidney Int. *91*, 575–586. https://doi.org/10.1016/j.kint.2016.10.039.

70. Sellmayr, M., Hernandez Petzsche, M.R., Ma, Q., Krüger, N., Liapis, H., Brink, A., Lenz, B., Angelotti, M.L., Gnemmi, V., Kuppe, C., et al. (2020). Only Hyperuricemia with Crystalluria, but not Asymptomatic Hyperuricemia, Drives Progression of Chronic Kidney Disease. J. Am. Soc. Nephrol. *31*, 2773–2792. https://doi.org/10.1681/ASN.2020040523.

71. Tao, J., Mariani, L., Eddy, S., Maecker, H., Kambham, N., Mehta, K., Hartman, J., Wang, W., Kretzler, M., and Lafayette, R.A. (2020). JAK-STAT Activity in Peripheral Blood Cells and Kidney Tissue in IgA Nephropathy. Clin. J. Am. Soc. Nephrol. *15*, 973–982. https://doi.org/10.2215/CJN.11010919.

72. Gluba, A., Banach, M., Hannam, S., Mikhailidis, D.P., Sakowicz, A., and Rysz, J. (2010). The role of Toll-like receptors in renal diseases. Nat. Rev. Nephrol. *6*, 224–235. https://doi.org/10.1038/nrneph.2010.16.

73. Wada, J., and Makino, H. (2016). Innate immunity in diabetes and diabetic nephropathy. Nat. Rev. Nephrol. *12*, 13–26. https://doi.org/10.1038/nrneph.2015.175.

74. Xu, Z., Zou, C., Yu, W., Xu, S., Huang, L., Khan, Z., Wang, J., Liang, G., and Wang, Y. (2019). Inhibition of STAT3 activation mediated by toll-like receptor 4 attenuates angiotensin II-induced renal fibrosis and dysfunction. Br. J. Pharmacol. *176*, 2627–2641. https://doi.org/10.1111/bph.14686.

75. Bai, J., Cervantes, C., Liu, J., He, S., Zhou, H., Zhang, B., Cai, H., Yin, D., Hu, D., Li, Z., et al. (2017). DsbA-L prevents obesity-induced inflammation and insulin resistance by suppressing the mtDNA release-activated cGAS-cGAMP-STING pathway. Proc. Natl. Acad. Sci. USA *114*, 12196–12201. https://doi.org/10.1073/pnas.1708744114.

76. Chung, K.W., Dhillon, P., Huang, S., Sheng, X., Shrestha, R., Qiu, C., Kaufman, B.A., Park, J., Pei, L., Baur, J., et al. (2019). Mitochondrial Damage and Activation of the STING Pathway Lead to Renal Inflammation and Fibrosis. Cell Metab. *30*, 784–799.e5. https://doi.org/10.1016/j.cmet.2019.08.003.

77. Hopfner, K.P., and Hornung, V. (2020). Molecular mechanisms and cellular functions of cGAS-STING signalling. Nat. Rev. Mol. Cell Biol. *21*, 501–521. https://doi.org/10.1038/s41580-020-0244-x.

78. Wilson, H.M., Reid, F.J., Brown, P.A., Power, D.A., Haites, N.E., and Booth, N.A. (1993). Effect of transforming growth factor-beta 1 on plasminogen activators and plasminogen activator inhibitor-1 in renal glomerular cells. Exp. Nephrol. *1*, 343–350.

79. Zhou, T., Luo, M., Cai, W., Zhou, S., Feng, D., Xu, C., and Wang, H. (2018). Runt-Related Transcription Factor 1 (RUNX1) Promotes TGF-beta-Induced Renal Tubular Epithelial-to-Mesenchymal Transition (EMT) and Renal Fibrosis through the PI3K Subunit p110delta. EBioMedicine *31*, 217–225. https://doi.org/10.1016/j.ebiom.2018.04.023.

80. Zhou, L., Li, Y., Zhou, D., Tan, R.J., and Liu, Y. (2013). Loss of Klotho contributes to kidney injury by derepression of Wnt/beta-catenin signaling. J. Am. Soc. Nephrol. *24*, 771–785. https://doi.org/10.1681/ASN.2012080865.

81. Tan, R.J., Zhou, D., Zhou, L., and Liu, Y. (2014). Wnt/beta-catenin signaling and kidney fibrosis. Kidney Int. Suppl. *4*, 84–90. https://doi.org/10.1038/kisup.2014.16.

82. Zhou, L., Li, Y., Hao, S., Zhou, D., Tan, R.J., Nie, J., Hou, F.F., Kahn, M., and Liu, Y. (2015). Multiple genes of the renin-angiotensin system are novel targets of Wnt/beta-catenin signaling. J. Am. Soc. Nephrol. *26*, 107–120. https://doi.org/10.1681/ASN.2014010085.

83. Xiao, L., Zhou, D., Tan, R.J., Fu, H., Zhou, L., Hou, F.F., and Liu, Y. (2016). Sustained Activation of Wnt/beta-Catenin Signaling Drives AKI to CKD Progression. J. Am. Soc. Nephrol. *27*, 1727–1740. https://doi.org/10.1681/ASN.2015040449.

84. Feng, Y., Ren, J., Gui, Y., Wei, W., Shu, B., Lu, Q., Xue, X., Sun, X., He, W., Yang, J., and Dai, C. (2018). Wnt/beta-Catenin-Promoted Macrophage Alternative Activation Contributes to Kidney Fibrosis. J. Am. Soc. Nephrol. *29*, 182–193. https://doi.org/10.1681/ASN.2017040391.

85. Luo, C., Zhou, S., Zhou, Z., Liu, Y., Yang, L., Liu, J., Zhang, Y., Li, H., Liu, Y., Hou, F.F., and Zhou, L. (2018). Wnt9a Promotes Renal Fibrosis by Accelerating Cellular Senescence in Tubular Epithelial Cells. J. Am. Soc. Nephrol. *29*, 1238–1256. https://doi.org/10.1681/ASN.2017050574.

86. Forrester, S.J., Booz, G.W., Sigmund, C.D., Coffman, T.M., Kawai, T., Rizzo, V., Scalia, R., and Eguchi, S. (2018). Angiotensin II Signal Transduction: An Update on Mechanisms of Physiology and Pathophysiology. Physiol.

Rev. *98*, 1627–1738. https://doi.org/10.1152/physrev.00038.2017.

87. Kalaitzidis, R.G., and Elisaf, M.S. (2018). Treatment of Hypertension in Chronic Kidney Disease. Curr. Hypertens. Rep. *20*, 64. https://doi.org/10.1007/s11906-018-0864-0.

88. Bielesz, B., Sirin, Y., Si, H., Niranjan, T., Gruenwald, A., Ahn, S., Kato, H., Pullman, J., Gessler, M., Haase, V.H., and Susztak, K. (2010). Epithelial Notch signaling regulates interstitial fibrosis development in the kidneys of mice and humans. J. Clin. Invest. *120*, 4040–4054. https://doi.org/10.1172/JCI43025.

89. Murea, M., Park, J.K., Sharma, S., Kato, H., Gruenwald, A., Niranjan, T., Si, H., Thomas, D.B., Pullman, J.M., Melamed, M.L., and Susztak, K. (2010). Expression of Notch pathway proteins correlates with albuminuria, glomerulosclerosis, and renal function. Kidney Int. *78*, 514–522. https://doi.org/10.1038/ki.2010.172.

90. Djudjaj, S., Chatziantoniou, C., Raffetseder, U., Guerrot, D., Dussaule, J.C., Boor, P., Kerroch, M., Hanssen, L., Brandt, S., Dittrich, A., et al. (2012). Notch-3 receptor activation drives inflammation and fibrosis following tubulointerstitial kidney injury. J. Pathol. *228*, 286–299. https://doi.org/10.1002/path.4076.

91. He, W., Wang, Y., Zhang, M.Z., You, L., Davis, L.S., Fan, H., Yang, H.C., Fogo, A.B., Zent, R., Harris, R.C., et al. (2010). Sirt1 activation protects the mouse renal medulla from oxidative injury. J. Clin. Invest. *120*, 1056–1068. https://doi.org/10.1172/JCI41563.

92. Shirazi, M.K., Azarnezhad, A., Abazari, M.F., Poorebrahim, M., Ghoraeian, P., Sanadgol, N., Bokharaie, H., Heydari, S., Abbasi, A., Kabiri, S., et al. (2019). The role of nitric oxide signaling in renoprotective effects of hydrogen sulfide against chronic kidney disease in rats: Involvement of oxidative stress, autophagy and apoptosis. J. Cell. Physiol. *234*, 11411–11423. https://doi.org/10.1002/jcp.27797.

93. Kim, I.Y., Lee, D.W., Lee, S.B., and Kwak, I.S. (2014). The role of uric acid in kidney fibrosis: experimental evidences for the causal relationship. BioMed Res. Int. *2014*, 638732. https://doi.org/10.1155/2014/638732.

94. Cecerska-Heryć, E., Heryć, R., Dutkiewicz, G., Michalczyk, A., Grygorcewicz, B., Serwin, N., Napiontek-Balińska, S., and Dołęgowska, B. (2022). Xanthine oxidoreductase activity in platelet-poor and rich plasma as a oxidative stress indicator in patients required renal replacement therapy. BMC Nephrol. *23*, 35. https://doi.org/10.1186/s12882-021-02649-8.

95. Taguchi, S., Nasu, T., Satoh, M., Kotozaki, Y., Tanno, K., Tanaka, F., Asahi, K., Ohmomo, H., Kikuchi, H., Kobayashi, T., et al. (2022). Association between Plasma Xanthine Oxidoreductase Activity and the Renal Function in a General Japanese Population: The Tohoku Medical Megabank Community-Based Cohort Study. Kidney Blood Press. Res. *47*, 722–728. https://doi.org/10.1159/000527654.

96. Davis, S., and Meltzer, P.S. (2007). GEOquery: a bridge between the Gene Expression Omnibus (GEO) and BioConductor. Bioinformatics *23*, 1846–1847. https://doi.org/10.1093/bioinformatics/btm254.

97. Barrett, T., Wilhite, S.E., Ledoux, P., Evangelista, C., Kim, I.F., Tomashevsky, M., Marshall, K.A., Phillippy, K.H., Sherman, P.M., Holko, M., et al. (2013). NCBI GEO: archive for functional genomics data sets–update. Nucleic Acids Res. *41*, D991–D995. https://doi.org/10.1093/nar/gks1193.

98. Parker, H.S., Leek, J.T., Favorov, A.V., Considine, M., Xia, X., Chavan, S., Chung, C.H., and Fertig, E.J. (2014). Preserving biological heterogeneity with a permuted surrogate variable analysis for genomics batch correction. Bioinformatics *30*, 2757–2763. https://doi.org/10.1093/bioinformatics/btu375.

99. Wang, L., Feng, Z., Wang, X., Wang, X., and Zhang, X. (2010). DEGseq: an R package for identifying differentially expressed genes from RNA-seq data. Bioinformatics *26*, 136–138. https://doi.org/10.1093/bioinformatics/btp612.

100. Yu, G., Wang, L.G., Han, Y., and He, Q.Y. (2012). clusterProfiler: an R package for comparing biological themes among gene clusters. OMICS *16*, 284–287. https://doi.org/10.1089/omi.2011.0118.

101. Wen, B., Mei, Z., Zeng, C., and Liu, S. (2017). metaX: a flexible and comprehensive software for processing metabolomics data. BMC Bioinf. *18*, 183. https://doi.org/10.1186/s12859-017-1579-y.

102. Tian, Y., Chen, L., and Jiang, Y. (2022). LASSO-based screening for potential prognostic biomarkers associated with glioblastoma. Front. Oncol. *12*, 1057383. https://doi.org/10.3389/fonc.2022.1057383.

103. Guo, L., Wang, Z., Du, Y., Mao, J., Zhang, J., Yu, Z., Guo, J., Zhao, J., Zhou, H., Wang, H., et al. (2020). Random-forest algorithm based biomarkers in predicting prognosis in the patients with hepatocellular carcinoma. Cancer Cell Int. *20*, 251. https://doi.org/10.1186/s12935-020-01274-z.

104. Di Guida, R., Engel, J., Allwood, J.W., Weber, R.J.M., Jones, M.R., Sommer, U., Viant, M.R., and Dunn, W.B. (2016). Non-targeted UHPLC-MS metabolomic data processing methods: a comparative investigation of normalisation, missing value imputation, transformation and scaling. Metabolomics *12*, 93. https://doi.org/10.1007/s11306-016-1030-9.

105. Dunn, W.B., Broadhurst, D., Begley, P., Zelena, E., Francis-McIntyre, S., Anderson, N., Brown, M., Knowles, J.D., Halsall, A., Haselden, J.N., et al. (2011). Procedures for large-scale metabolic profiling of serum and plasma using gas chromatography and liquid chromatography coupled to mass spectrometry. Nat. Protoc. *6*, 1060–1083. https://doi.org/10.1038/nprot.2011.335.

106. Wishart, D.S., Guo, A., Oler, E., Wang, F., Anjum, A., Peters, H., Dizon, R., Sayeeda, Z., Tian, S., Lee, B.L., et al. (2022). HMDB 5.0: the Human Metabolome Database for 2022. Nucleic Acids Res. *50*, D622–D631. https://doi.org/10.1093/nar/gkab1062.

107. Kanehisa, M., Furumichi, M., Sato, Y., Ishiguro-Watanabe, M., and Tanabe, M. (2021). KEGG: integrating viruses and cellular organisms. Nucleic Acids Res. *49*, D545–D551. https://doi.org/10.1093/nar/gkaa970.

STAR★METHODS

KEY RESOURCES TABLE

REAGENT or RESOURCE	SOURCE	IDENTIFIER
Chemicals, peptides, and recombinant proteins		
Fetal bovine serum	Gibco Thermo Fisher Scientific	10099141C
DMEM/F12	Gibco Thermo Fisher Scientific	Cat# C11330500BT
Trypsin	Gibco Thermo Fisher Scientific	Cat# 25200056
rhTGF-β1 (10 μg)	R&D Systems	Cat# 240-B-010
Critical commercial assays		
TRIzol	TAKARA	108-95-2
HiScript II Q RT SuperMix	Vazyme	R222-01
SYBR Green PCR mix	Vazyme	Q131-02
Human XOR Assay Kit (Colorimetric method)	XLPCC	XL-SH210
Human XO Assay Kit	XLPCC	XL-SH212
Human NLRP3 ELISA Kit	XLPCC	XL-EH1894
Deposited data		
Metabolomics data	https://www.ebi.ac.uk/metabolights/	MTBLS142
Experimental models: Cell lines		
Human renal tubular cell line HK2	ATCC	CRL-2190
Oligonucleotides		
Human XOR detection primers Forward Primer 5′-GGACAGTTGTGGCTCTTGAGGT-3′ Reverse Primer 5′-GGAAGGTTGGTTTTGCACAGCC-3′	PrimerBank	Figure 5
Human XDH detection primers Forward Primer 5′-ACCCCGTGTTCATGGCCAGTG-3′ Reverse Primer 5′-TCCGGGAGGCCTGCTTGAATG-3′	PrimerBank	Figure 5
Human ROMO1 detection primers Forward Primer 5′-AAGCTGCTTCGACCGTGTC-3′ Reverse Primer 5′-CCCGCATTCCGATCCTGAG-3′	PrimerBank	Figure 5
Human NOA1 detection primers Forward Primer 5′-CCTTCCAGCACTCATCGAGTC-3′ Reverse Primer 5′-TCCAGGATGTACTCCGGGAAC-3′	PrimerBank	Figure 5
Human COX-2 detection primers Forward Primer 5′-TAAGTGCGATTGTACCCGGAC-3′ Reverse Primer 5′-TTTGTAGCCATAGTCAGCATTGT-3′	PrimerBank	Figure 5
Human NF-κB detection primers Forward Primer 5′-AACAGAGAGGATTTCGTTTCCG-3′ Reverse Primer 5′-TTTGACCTGAGGGTAAGACTTCT-3′	PrimerBank	Figure 5
Human GAPDH detection primers Forward Primer 5′-GGAGCGAGATCCCTCCAAAAT-3′ Reverse Primer 5′-GGCTGTTGTCATACTTCTCATGG-3′	PrimerBank	Figure 5
Software and algorithms		
GraphPad Prism 9 software	GraphPad software	https://www.graphpad.com
GEOquery	Davis et al.[96] and Barrett et al.[97]	bioconductor.org/packages/release/bioc/html/GEOquery.html
combat	Parker et al.[98]	ComBat function - RDocumentation

(*Continued on next page*)

Continued

REAGENT or RESOURCE	SOURCE	IDENTIFIER
DEGseq	Wang et al.[99]	bioconductor.org/packages/release/bioc/html/DEGseq.html
clusterProfiler	Yu et al.[100]	bioconductor.org/packages/release/bioc/html/clusterProfiler.html
Q exactive HF	Bo Wen et al.[101]	Q Exactive HF Hybrid Quadrupole Orbitrap Mass Spectrometer Support | Thermo Fisher Scientific - CN

RESOURCE AVAILABILITY

Lead contact

Further information, requests, and inquiries should be directed to and will be fulfilled by the Lead Contact, Donghui Zheng (zddwjj@126.com).

Material availability

The study did not generate new unique reagents.

Data and code availability

Metabolomics data have been deposited at MetaboLights (https://www.ebi.ac.uk/metabolights/) and are publicly available as of the date of publication. Accession numbers are listed in the key resources table. This paper does not report original code.

EXPERIMENTAL MODEL AND STUDY PARTICIPANT DETAILS

Human participants

A total of 121 Han Chinese participants in the affiliated Huai'an Hospital of Xuzhou Medical University were enrolled in this study, and the patient profiles are shown in Table 1 and Figure 1A. The causes of all CKD patients enrolled were analyzed in Table 2, and the urinary examination was performed in all participants. Firstly, midstream urine of all patients seeking treatment in the nephrology department were collected and examined by the dry chemical strip method (Sysmex UC-3500), the patients with urinary occult blood or urinary protein being 1+ or above were identified and their eGFR were calculated. Next, other CKD patients with renal damage or decreased renal function for no less than three months (2012 The lancet) were identified based on the results of hematology and imaging examination. All CKD patients were diagnosed with CKD according to the *2017 Guidelines for Screening, Diagnosis, and Prevention of Chronic Kidney Disease*. The exclusion criteria were incomplete clinical information, those who used XOR inhibitor, corticosteroid and hyperuricemia patients, those who had severe malnutrition, and those with eGFR <30 mL/(min·1.73 m2). eGFR is used universally as a screening tool to determine the stage of CKD.[49]

Ethical approval

The study was conducted in accordance with the guidelines of the Declaration of Helsinki (1991), and approved by the Ethics Committee of the Affiliated Huai'an Hospital of Xuzhou Medical University (HEYLL201883).

Consent for publication

This research has consent to study and publish. In addition, the consents are kept in The Affiliated Huai'an Hospital of Xuzhou Medical University's archives.

Cell

The human renal tubular cell line HK2, which has been authenticated, was purchased from American Type Culture Collection (ATCC, Manassas, VA, RRID: CVCL_0302), and screened regularly for mycoplasma contamination. HK2 cells were cultured in DMEM/F12 supplemented with 10% fetal bovine serum (GIBCO, 10099141C, Australia), and were incubated in a humidified incubator of 5% CO_2 at 37°C.

METHOD DETAILS

Plasma XOR activity

Plasma XOR activity was measured by UA production from XOR. A serum separator tube was used to store the patients' blood at 4°C overnight before centrifugation for 20 minutes at 1000×*g*. Then, the serum was maintain at −80°C until measuring using an assay kit (Colorimetric Method) from XLPCC, China.

Sample selection, data acquisition, and processing

The expression profile datasets GSE15072, GSE45980, GSE66494, GSE69438, and GSE70528 were downloaded from GEO (https://www.ncbi.nlm.nih.gov/geo/) database using the GEOquery package.[96,97] GSE15072 and GSE70528 were collected from peripheral blood. GSE45980, GSE69438 and GSE70528 were collected from renal biopsy. The detailed information of these microarray datasets is listed in Figure 3A. Raw data of the merged datasets were removed the inter-batch difference using the combat package.[98] Differentially expressed genes were identified using DEGseq[99] with the p-value <0.05 and |log2FC| >1.5. KEGG pathway enrichment analyses of DEGs were preformed using clusterProfiler package.[100]

Identification of hub CKD genes

Differentially expressed matrices of GEO datasets were used to identify the hub CKD genes by merging machine learning including LASSO logistic regression[102] and random-forest algorithm.[103] The LASSO algorithm was applied with running 10-fold cross-validation for 1,000 cycles on minimum criteria and 1-s.e. criteria. The important variables were selected by random-forest algorithm with minimum error regression trees and ranked using IncNodePurity by using random-forest package. Ultimately, we combined the genes from both LASSO and RF algorithms for further analysis.

Constructing samples induced by TGFβ

HK2 cells were cultured in DMEM/F12 supplemented with 10% fetal bovine serum, and then stimulated with 10 ng/mL TGF-β1 (R&D Systems, Minneapolis, MN) for 24 hours. The obtained samples were prepared for extracting RNA for quantitative real-time PCR and metabolite extraction.

Quantitative real-time PCR (qRT-PCR)

TRIzol (TAKARA, SD412) was used to obtain whole RNA from HK2 cells. Then, the first-strand cDNAs were synthesized from 1 μg of total RNA in a 20 μL reaction with HiScript II Q RT SuperMix for qPCR (Vazyme, R222-01) following the manufacturer's instructions. Quantitative real-time PCR used SYBR Green PCR mix (Vazyme, Q131-02). Primers were synthesized by Tsingke Biotechnology Co (China, Beijing), and the sequences are listed in key resources table. The PCR cycling condition was 50°C for 15 minutes and 60°C for 15 seconds. Gapdh was selected as an internal control. Based on threshold cycle values (ΔCt), mRNA expression was analyzed, then converted to fold changes using $2^{-\Delta\Delta Ct}$ method.

Metabolite extraction, UPLC-MS analysis, and metabolite identification

A total of 25 mg samples of control and TGFβ were added into 2-mL thickened centrifuge tubes with adding magnetic beads and 10 μL prepared internal standard. Then, the samples were ground for 5 minutes with 50 Hz after adding 800 μL precooled extraction reagent including 300 μL methanol, 300 μL acetonitrile, and 200 μL water, and stored at −20°C for 2 hours. Next, 600 μL of the samples was collected and preserved by freezing and then drying after centrifuging at 25,000 × *g* for 15 minutes at 4°C. The dried samples were completely dissolved with 120 μL of 50% methanol and centrifuged at 25,000 × *g* for 15 minutes at 4°C. The supernatant with mixing QC samples was prepared for LC-MS/MS.

In this study, Q exactive HF (Thermo Fisher Scientific, USA) was used for mass spectrometry data acquisition with primary and secondary levels. The full scan range was set at 70–1050 m/z, and the top three precursors were selected for subsequent MS/MS. The resolution, automatic gain control (AGC), and maximum ion injection time were set at 120,000, 3e6, and 100 ms, respectively (primary level), and 30,000, 1e5, and 50 ms, respectively (secondary level).

Raw data collected by LC-MS/MS were inserted to compound discoverer 3.3 (Thermo Fisher Scientific, USA) software and annotated by BGI metabolome (https://www.bgi.com/global/service/targeted-metabolomics), mzcloud (https://www.mzcloud.org/), and chemspider database (https://www.chemspider.com). The data matrix containing metabolite peak area and identification results was obtained

with the following parameters: parent ion mass deviation <5 ppm, mass deviation of fragment ions <10 ppm, and retention time deviation <0.2 min.

Data preprocessing, quality control, and screening for the differential metabolites

By applying MetaX,[101] the data matrix was prepared for data preprocessing including normalizing data by probabilistic quotient normalization (PQN),[104] correcting batch effect by quality control-based robust LOESS signal correction (QC-RLSC),[105] and removing metabolites with a coefficient of variation larger than 30% on their relative peak area in QC samples. Principal component analysis (PCA) was used to determine whether QC samples and experiment samples were aggregated. The Human Metabolome Database[106] and Kyoto Encyclopedia of Genes and Genomes (KEGG)[107] were used to search metabolic pathways. Differential metabolites were screened with the following criteria: fold change ≥ 1.5 or ≤ 0.66 and p-value <0.05.

QUANTIFICATION AND STATISTICAL ANALYSIS

Statistical analysis

All clinical data statistical tests were conducted in Prism 9 software. Quantitative normally distributed data were expressed as the means $\pm$ standard deviations (SDs). A nonparametric test was used to explore the effect of XOR on kidney function. A p-value <0.05 was considered statistically significant. The gene expression measured by RNA-seq was analyzed using the Student's *t* test. Asterisks and ns indicate significant and nonsignificant differences between the groups, respectively. A p-value <0.05 was considered statistically significant.